

SCIENTIFIC REPORTS

OPEN

Plac1 Is a Key Regulator of the Inflammatory Response and Immune Tolerance In Mammary Tumorigenesis

Hongyan Yuan¹, Xiaoyi Wang¹, Chunmei Shi¹, Lu Jin¹, Jianxia Hu², Alston Zhang¹, James Li³, Nairuthya Vijayendra¹, Venkata Doodala¹, Spencer Weiss¹, Yong Tang¹, Louis M. Weiner¹ & Robert I. Glazer¹

Plac1 is an X-linked trophoblast gene expressed at high levels in the placenta, but not in adult somatic tissues other than the testis. Plac1 however is re-expressed in several solid tumors and in most human cancer cell lines. To explore the role of Plac1 in cancer progression, Plac1 was reduced by RNA interference in EO771 mammary carcinoma cells. EO771 “knockdown” (KD) resulted in 50% reduction in proliferation *in vitro* and impaired tumor growth in syngeneic mice; however, tumor growth in SCID mice was equivalent to tumor cells expressing a non-silencing control RNA, suggesting that Plac1 regulated adaptive immunity. Gene expression profiling of Plac1 KD cells indicated reduction in several inflammatory and immune factors, including Cxcl1, Ccl5, Ly6a/Sca-1, Ly6c and Lif. Treatment of mice engrafted with wild-type EO771 cells with a Cxcr2 antagonist impaired tumor growth, reduced myeloid-derived suppressor cells and regulatory T cells, while increasing macrophages, dendritic cells, NK cells and the penetration of CD8+ T cells into the tumor bed. Cxcl1 KD phenocopied the effects of Plac1 KD on tumor growth, and overexpression of Cxcl1 partially rescued Plac1 KD cells. These results reveal that Plac1 modulates a tolerogenic tumor microenvironment in part by modulating the chemokine axis.

Placental-specific protein 1 (Plac1) is an Xq26-linked gene that encodes a microvillous membrane protein expressed primarily in trophoblasts, at low levels in the testis, but not in other adult somatic tissues¹, and has the most restricted normal tissue expression pattern in comparison to other cancer/testis antigens². Silva first reported that Plac1 RNA was expressed over a 4-log range in >50% of human cancer cell lines covering 17 different malignancies², suggesting that some cancers mirror an onco-placental disease or a “somatic cell pregnancy”³. This hypothesis has been confirmed by the detection of Plac1 in malignancies of the breast^{4–6}, endometrium⁷, ovary⁷, lung^{2,8}, liver⁹, colon^{6,10,11}, stomach¹² and prostate¹³. In colorectal cancer biopsies, higher levels of Plac1 were detected in 50% of stage III/IV disease in comparison to early stage disease^{9,10}, and Plac1-dependent cytotoxic T cell (CTL) activity correlated with overall survival¹¹.

In the MMTV-PPARd transgenic model of luminal B breast cancer, Plac1 expression was highly elevated at the onset and throughout mammary tumorigenesis¹⁴, suggesting that it might have a role in the initiation and progression of tumor development. Previous studies found that Plac1 transcription in human breast cancer cells was regulated by many of the same co-activators associated with PPARd and other nuclear receptors^{15–17}, including C/EBPβ and NCOA3^{18,19}, both of which have been implicated in breast cancer progression^{16,20–22}. Despite these findings, little is known about the oncogenic processes downstream of Plac1. To address this question, EO771 mammary carcinoma cells, which express high levels of Plac1, were used to examine gene expression and signaling pathways under the control of Plac1. Our findings reveal that Plac1 regulates a chemokine and immune tolerogenic signaling network necessary for sustaining tumor growth, which suggests potential therapeutic strategies that could alter the tumor microenvironment to make it more amenable to therapy.

¹Department of Oncology and Lombardi Comprehensive Cancer Center, Georgetown University, Washington, DC, 20007, USA. ²Laboratory of Thyroid Diseases, the Affiliated Hospital of Qingdao University, Qingdao, 266003, China. ³Department of Bioinformatics, Biostatistics and Biomathematics, Georgetown University Medical Center, Washington, DC, 20007, USA. Correspondence and requests for materials should be addressed to R.I.G. (email: glazerr@georgetown.edu)

Gene	Raw Score		shPlac1/Scr	Function
	Scr	shPlac1		
Cxcl1	7054	106	−67	Cxcr2 ligand
Ccl7	2854	153	−19	Ccr3 ligand
CD68	931	55	−18	Macrophage phagocytosis
Ccl2	3640	305	−12	Ccr2/Ccr5 ligand; MDSC
Lif	664	80	−8.3	Immune tolerance at maternal–fetal interface
C1	918	128	−7.1	Complement
Ccl5	3812	784	−4.9	Ccr1/3/4/5 ligand
Tsc22d3	2265	478	−4.8	Mediates IL10 immunosuppression
Ly6a	4937	1160	−4.3	Sca-1; inhibits TGF β , Pten and PPAR γ
Ly6c	1198	329	−3.7	Mono/M ϕ marker; MDSC
Clec2d	366	99	−3.7	Protects against NK cells
Cxcl10	459	130	−3.6	Cxcr3 ligand
CD274	302	91	−3.4	PD-L1; PD-1 ligand

Table 1. Expression of immune-related genes in EO771/shPlac1 cells. Shown are ≥ 3.0 -fold changes in expression with a raw score ≥ 300 in either EO771/shPlac1 or EO771/Scr cells.

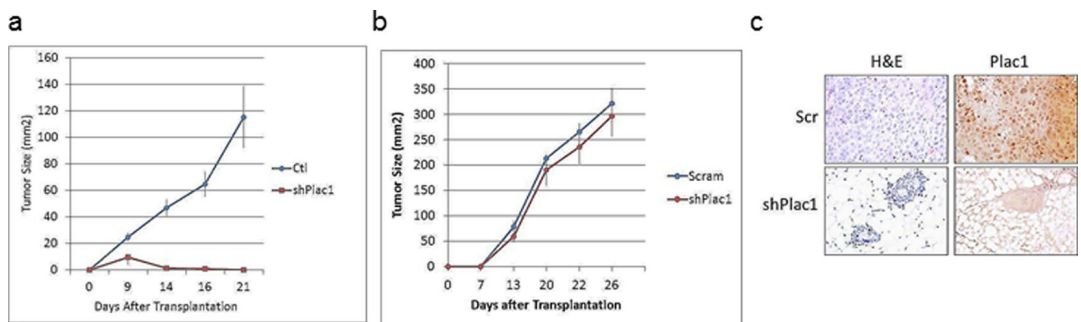


Figure 2. Growth of EO771/Scr and EO771/shPlac1 cells in syngeneic and SCID mice. (a) Syngeneic C57BL/6 mice or (b) SCID mice at five weeks of age, were inoculated in the mammary gland with 1×10^6 cells. Tumor size was measured by calipers in two dimensions. Tumor growth for EO771/Scr and EO771/shPlac1 cells in syngeneic mice differed significantly ($P = 0.040$) by the unpaired Student's t test. There was no significant difference ($P > 0.05$) in tumor growth between the two cell lines in SCID mice. Shown is the mean \pm SD, $N = 5$ per group. (c) H&E staining and Plac1 IHC in isografts of EO771/Scr and EO771/shPlac1 cells. Magnification 400X.

per week with vehicle or 2 or 20 mg/kg SB225002 beginning 10 days after transplantation (Fig. 3a). Whereas, the lower dose partially inhibited tumor growth, 20 mg/kg SB225002 completely blocked growth after a lag of two weeks. Tumor stasis at 17 days following cell inoculation was associated with reduction in expression of immune and chemokine genes, many of which were downregulated in EO771/shPlac1 cells (Fig. 3b). Cell sorting of tumor immune infiltrates indicated that SB225002 treatment reduced myeloid-derived suppressor cells (MDSC) and Treg cells, and increased CD8 $^+$ /CD4 $^+$ T cells, NK cells, macrophages and dendritic cells (Fig. 3c,d). Especially noteworthy was the greater infiltration of CD8 $^+$ T cells into the tumor bed following SB225002 treatment (Fig. 3e), which was accompanied by increased macrophage and Treg cell infiltration, reduction of Plac1 and increased apoptosis (Fig. 3f). Since we did not determine tissue levels of SB225002, we determined its cytotoxicity in EO771 cell culture (Supplementary Fig. 2). SB225002 at concentration less than 100 nM were not cytotoxic, but produced cytotoxicity at concentrations exceeding 1000 nM. Since we have not carried out pharmacokinetics, the contribution of SB225002 cytotoxicity to its antitumor effect cannot be ascertained.

Cxcl1 reduction inhibits tumor growth and immune cell-related transcription. To evaluate the role of Cxcl1/Cxcr2 signaling in tumor growth, EO771 cells were transduced with scrambled shRNA (Scr) or four Cxcl1 shRNAs (Fig. 4a). EO771 cells expressing sh174 (*shCxcl1*) exhibited $>95\%$ reduction of Cxcl1 RNA expression. After 48 hr in monolayer culture, EO771/shCxcl1 cells grew at approximately 30% of the rate of control cells (Scr) (Fig. 4b). Comparison of the gene expression profile of EO771/shCxcl1 cells with EO771/Scr cells revealed a small subset of genes with ≥ 3 -fold changes, including Ly6a, IL23a, C3, Cxcl1 and CD68 (Table 2, Supplementary Table 3). Transplantation of EO771/shCxcl1 cells into syngeneic mice resulted in impaired tumor growth in comparison to control cells (Fig. 4c), a result that was similar to EO771/shPlac1 cells (Fig. 2a). Changes in immune-related gene expression (Table 2) were confirmed by qRT-PCR, with the exception of CD68, which

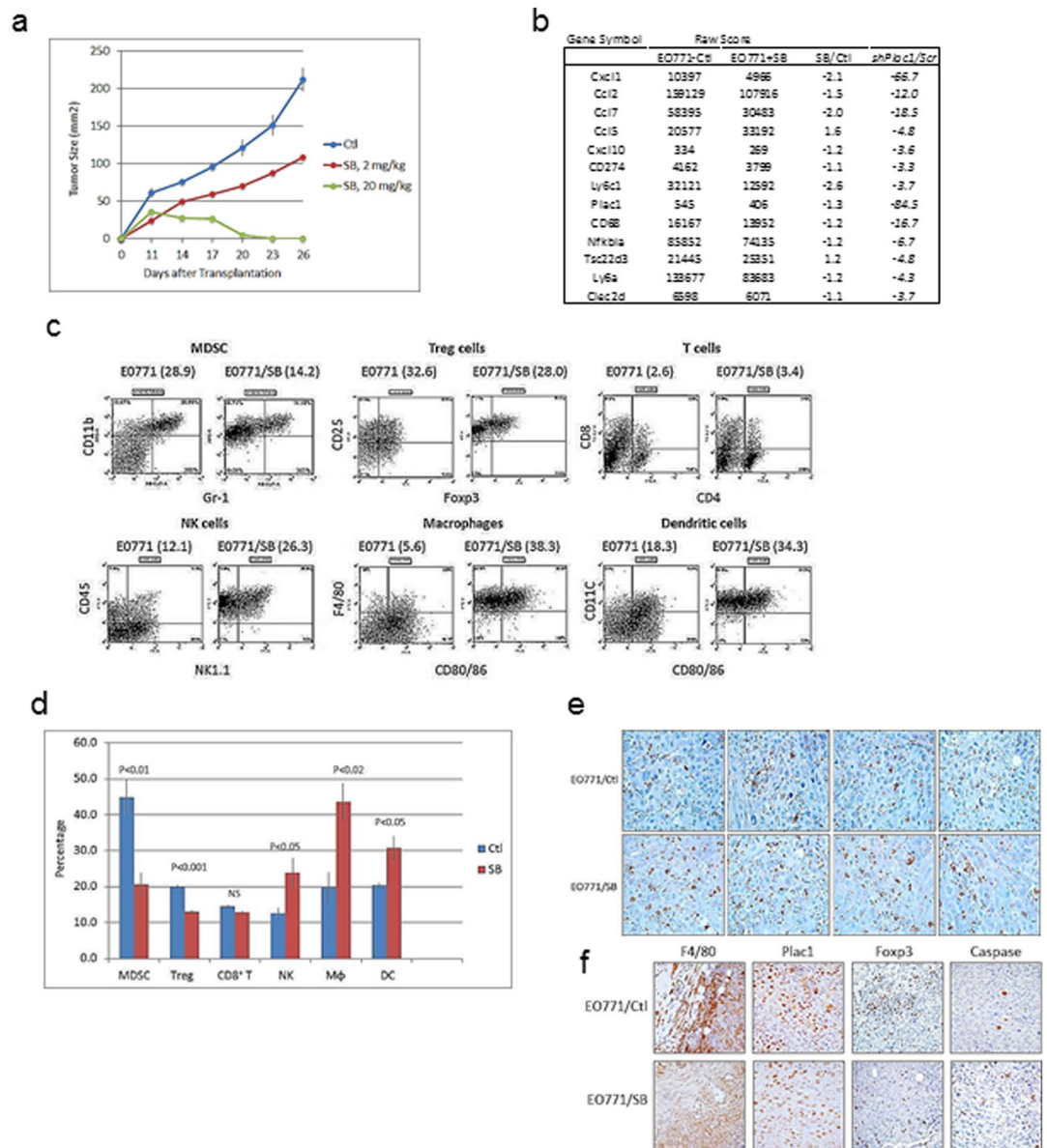


Figure 3. Growth of EO771 cells in syngeneic mice following treatment with a Cxcr₂ antagonist. **(a)** Syngeneic 57BL/6 mice were inoculated in the mammary gland with 1×10^6 at five weeks of age, and injected i.p. daily with vehicle (blue) or 2 mg/kg (red) or 20 mg/kg (green) SB225002 beginning 11 days after cell inoculation. SB225002 completely suppressed tumor growth after 14 days. Differences between vehicle- and 2 mg/kg SB225002-treated mice were not significantly different ($P = 0.145$); differences between vehicle- and 20 mg/kg SB225002-treated mice were significantly different ($P = 0.005$) by the unpaired two-tailed Student's *t* test. Shown is the mean \pm SD, $N = 5$ per group. **(b)** Immune gene expression in tumors 17 days after treatment with 20 mg/kg SB225002. Shown is the relative expression in control and SB225002-treated mice in comparison to their changes in EO771/shPlac1 cells (Table 1). **(c)** FACS analysis of immune cell tumor infiltrates in isografts after treatment with vehicle or SB225002 as in **(b)**. SB225002 treatment reduced the percentage of immune cell tumor infiltrates of CD11b⁺/Gr-1⁺ myeloid-derived suppressor cells (MDSC) and Foxp3⁺/CD25⁺ T cells (Treg), and increased the percentages of CD8⁺/CD4⁺ T cells (T), CD3⁺/NK1.1⁺ NK cells (NK) and F4/80⁺/CD80/86⁺ macrophages (Mφ) and CD11c⁺/CD80/86⁺ dendritic cells (DC). Numbers in parentheses () represent the percentages of each cell population. **(d)** Bar graph represents the mean \pm SD of the percent distribution of immune cell tumor infiltrates as in **(c)**; *P* values were determined by the unpaired two-tailed Student's *t* test, $N = 4$ per group. **(e)** CD8⁺ T cell infiltration determined by IHC in tumor isografts from vehicle-treated (EO771/Ctl) and SB225002-treated (EO771/SB) mice. Infiltration of CD8⁺ T cells increased after treatment with 20 mg/kg SB225002. Magnification 600X. **(f)** Macrophage (F4/80) and Treg cell (Foxp3) infiltration, Plac1 expression and apoptosis by cleaved caspase-3 expression (Caspase) in tumor isografts from vehicle-treated (EO771/Ctl) and SB225002-treated (EO771/SB) mice. Infiltration of macrophages and Treg cells were reduced and apoptosis was increased after treatment with 20 mg/kg SB225002. Magnification 400X.

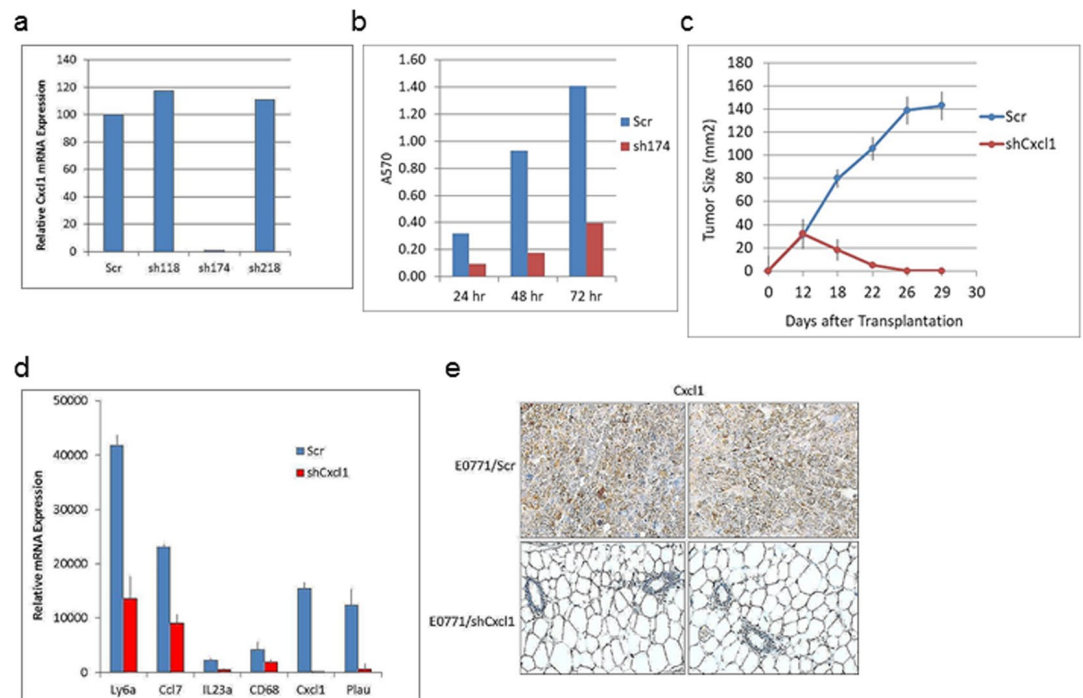


Figure 4. Lentivirus-mediated reduction of Cxcl1 in EO771 cells. **(a)** EO771 cells were transduced with lentiviruses expressing scrambled RNA (Scr) or three Cxcl1 shRNAs designated sh118, sh174, sh218; sh174 inhibited RNA expression >99% (EO771/shCxcl1). **(b)** EO771/Scr and EO771/shCxcl1 cells were grown as monolayers, and the number of viable cells were determined by sulforhodamine B staining. Shown is the mean \pm S.D. of triplicate analysis from three samples, which were significantly different ($P < 0.001$) by the two-tailed Student's *t* test. **(c)** Growth of EO771/Scr and EO771/shCxcl1 cells in syngeneic mice. Mice at five weeks of age were inoculated in the mammary gland with 1×10^6 cells, and tumor size was measured by calipers in two dimensions. Differences in tumor growth between EO771/Scr and EO771/shCxcl1 cells were significantly different ($P = 0.006$) by the unpaired two-tailed Student's *t* test; $N = 5$. **(d)** qRT-PCR analysis of genes downregulated in EO771/shCxcl1 cells. Shown is the mean \pm SD of triplicate analysis of 3 samples. Significant differences between EO771/Scr and EO771/shCxcl1 cells were obtained for Plau ($P < 0.02$), C3 ($P < 0.01$), Ly6a ($P < 0.01$), Ccl7 ($P < 0.001$) and Il23a ($P < 0.01$) by the two-sided Student's *t* test; differences for CD68 were not significantly different ($P > 0.05$).

Gene	log 2		Raw Score		shCxcl1/Scr
	Scr	shCxcl1	Scr	shCxcl1	
Ly6a	12.93	11.29	7787	2512	-3.1
Il23a	8.84	7.06	459	133	-3.5
C3	8.48	6.55	358	94	-3.8
Cxcl1	11.06	9.07	2137	536	-4.0
CD68	8.62	6.54	394	93	-4.2

Table 2. Expression of immune-related genes in EO771/shCxcl1 cells. Shown are ≥ 3 -fold changes in gene expression with a raw score ≥ 300 in EO771/shCxcl1 or EO771/Scr cells.

did not change significantly (Fig. 4d). Measurement of Cxcl1 in tumors or mammary tissue by IHC after 21 days indicated the presence of Cxcl1 in EO771/Scr tumors, but not in EO771/shCxcl1 engrafted mammary tissue (Fig. 4e). Comparison of gene expression in EO771/shPlac1 vs. EO771/shCxcl1 cells indicated reduced expression in five genes in common, viz. CD68, Cxcl1, Ly6a, Plau and Rgs16 (Table 3), although CD68 was not changed significantly in EO771/shCxcl1 cells as measured by qRT-PCR (Fig. 4d).

Cxcl1 partially rescues Plac1 reduction in EO771 cells. To determine the contribution of Cxcl1 to the effects of Plac1 downregulation on tumor growth, EO771/sh490 cells were transduced with a retrovirus expressing Cxcl1-mCherry and EO771/Scr and EO771/sh490 were transduced with mCherry alone (Fig. 5). After selection in G418, a significant percentage of cells co-expressed GFP and mCherry (Fig. 5a) and Cxcl1 mRNA (Fig. 5b). The growth of EO771/sh490 cells *in vitro* was slower rate than control cells as shown in Fig. 1c, but cells expressing Cxcl1 largely rescued this effect (Fig. 5c). Isografts of these cell lines in syngeneic mice confirmed the

Gene	shPlac1/Scr	shCxcl1/Scr
CD68	−4.2	−4.2
Cxcl1	−67	−4.0
Ly6a	−4.3	−3.1
Plau	−7.1	−7.3
Rgs16	−7.7	−3.2

Table 3. Gene expression common to EO771/shPlac1 and EO771/shCxcl1 cells. Shown is the ratio between EO771/shPlac1 or EO771/shCxcl1 cells to EO771/Scr control cells for genes with ≥ 3.0 -fold changes in expression and a raw score ≥ 300 .

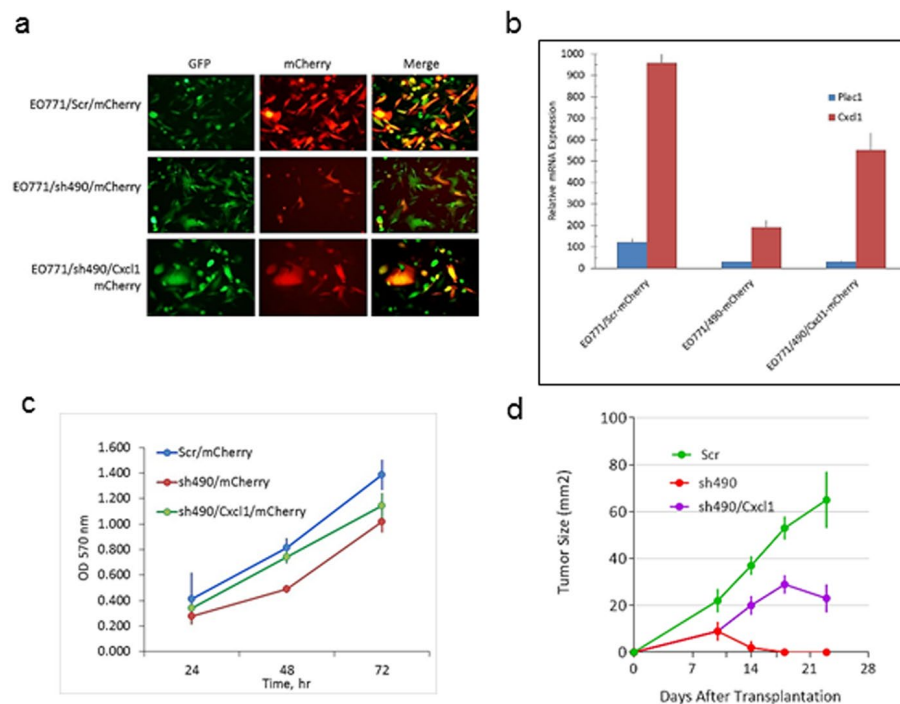


Figure 5. Cxcl1 rescue of EO771/sh490 cells. (a) EO771/Scr and EO771/sh490 cells expressing eGFP were transduced with a lentivirus expressing Cxcl1 and mCherry, and selected for 35 days in 3.5 mg/ml G418. The merged photo shows cells co-expressing eGFP and mCherry (yellow). Magnification 200X. (b) qRT-PCR for Plac1 and Cxcl1 in EO771/Scr, EO771/sh490 and EO771/sh490/Cxcl1 cells. Shown is the mean \pm S.D. of triplicate determinations. (c) EO771/sh490/Cxcl1 cells were grown in 96-well plates at an initial density of 5,000 cells per well in media supplemented with 3.5 mg/ml G418. Cell density was determined by sulforhodamine B staining. Shown is the mean \pm SD of triplicate determinations. (d) Syngeneic C57BL/6 mice were inoculated in the mammary gland with 1×10^6 at five weeks of age. There was a significant difference in the growth EO771/sh490 cells ($P = 0.021$) and EO771/sh490/Cxcl1 cells ($P = 0.034$) vs. EO771/Scr cells by the unpaired two-tailed Student's *t* test. Shown is the mean \pm SD, $N = 6$ per group.

poor growth of EO771/sh490 cells, and further showed that Cxcl1 could partially rescue their poor tumorigenicity (Fig. 5d).

As an added proof of the function of Plac1 in tumorigenesis, MC cells, a cell line with low Plac1 expression (Fig. 1a), were transfected with Plac1 (Supplementary Fig. 3, Supplementary Table 5). MC/Plac1 cells grew at a higher rate than control cells and exhibited less apoptosis, and upregulated a gene expression profile that included several of the chemokines as well as CD274 that were downregulated in EO771/shPlac1 cells.

Discussion

The present study establishes the first link between the trophoblast gene, Plac1, and adaptive immunity, through its ability to modulate chemokine expression and other immune cell regulators. In retrospect, this is not too surprising since the placenta may be regarded as a foreign allograft protected from host vs. graft rejection²³ in part by the presence of Treg cells in the uterine decidua²⁴. However, the link between Plac1, chemokine signaling and immune tolerance in tumors is a novel and relevant finding since the latter processes are hallmarks of most, if not all, solid tumors^{25,26}. The relevance of Plac1 to mammary tumorigenesis was first noted in MMTV-PPAR α mice, where Plac1 was markedly upregulated at the onset and throughout tumor development¹⁴. This finding implicated

nuclear receptor signaling in the transcriptional regulation of *Plac1*, as noted previously for its activation at alternate promoter regions in the *Plac1* locus by LXR and RXRA²⁷. However, from a mechanistic perspective, the downstream intracellular components interacting with *Plac1* have not been determined. *Plac1* is predominantly extracellular with an N-terminal signal peptide, a small transmembrane domain and an extracellular ZP3 domain²⁸, which promotes protein-protein interactions. By analogy, cytokine receptors lacking an intracellular signaling domain partner with co-receptors, adapter molecules and cytosolic protein tyrosine kinases to effect signaling²⁹, and such a mechanism may also pertain to *Plac1*.

In the present study, the panel of immune-related genes down-regulated by *Plac1* 'knockdown' (Table 1) suggest that one of its functions is to modulate chemokine effector pathways associated with immune evasion, such as antigen presentation, angiogenesis and myeloid cell, T cell and fibroblast activation (see scheme in Supplementary Fig. 4). One dominant downstream effector pathway was the *Cxcl1/Cxcr2* axis, as shown by inhibition of tumor growth by the *Cxcr2* antagonist SB25002 (Fig. 3a), and the inability of EO771/sh*Cxcl1* cells to sustain tumor proliferation in syngeneic mice (Fig. 4c). Inhibition of *Cxcr2* by SB25002 was associated with reduction of Treg cells and MDSC, and an increasing the percentage of CD8⁺ T cells, macrophages, NK cells and dendritic cells, which was consistent with previous studies demonstrating the ability of SB225002 to suppress MDSC infiltration in breast tumor xenografts³⁰ and prostate tumors³¹, as well as metastasis via S100A8/A9³⁰. Thus, our data suggest that one role of *Plac1* may be to maintain the production of inflammatory and immunoregulatory chemokines to effect changes in the stromal microenvironment conducive to immune tolerance and poor outcome^{30,32,33}, which would explain the poor tumorigenicity of EO771/sh*Plac1* cells in syngeneic mice, but not in SCID mice. Although, co-expression of *Plac1* and *Cxcl1* in breast cancer tissue has not been reported, *Cxcl1* expression in breast cancer biopsies was found to be elevated in metastases, and inversely related to ER α expression and relapse-free survival³⁴.

Despite focusing on the immunological aspects of *Plac1* function, it was apparent that it affected several signaling pathways in EO771 cells (Supplementary Table 2). Changes in gene expression common to both EO771/sh*Plac1* and EO771/sh*Cxcl1* cells, apart from *Cxcl1*, included reduced expression of *Plau*, *Ly6a*, *CD68* and *Rgs16* (Table 3). *Plau* is a well-known marker of metastasis³⁵, and its role in invasion has been noted in trophoblast migration³⁶. *Ly6a/Sca-1* is a mouse stem cell and tumor-initiating cell biomarker^{37,38} that down-regulates several tumor suppressor pathways, including PPAR γ , TGF- β and PTEN^{39,40}. *CD68* is a scavenger receptor involved in phagocytosis, particularly in M2 polarized macrophages⁴¹, and has been implicated in immunotolerance by tumor-associated macrophages⁴². *Rgs16* is a G-protein-coupled receptor associated with vascular smooth muscle cell proliferation and angiogenesis, which play prominent roles in oncogenesis⁴³. Thus, the functions of *Plac1* in placental development⁴⁴ appear to phenocopy its functions in tumorigenesis, which supports the onco-placental nature of cancer³. From a therapeutic perspective, our data not only suggest that *Plac1* may be a potential drug target, but that chemokine receptor antagonists developed for chronic inflammatory disorders, including COPD and psoriasis^{45,46}, may be useful adjuvants when used in combination with other therapies to enhance the efficacy of cancer treatment^{47,48}.

Methods

Cell lines. EO771 cells were originally isolated from a spontaneous mammary carcinoma in C57BL/6 mice⁴⁹, and were provided by Dr. Louis M. Weiner, Georgetown University. EO771 cells tested negative against the IMPACT II panel of infectious agents (IDEXX). *Plac1* and *Cxcl1* expression were reduced with the piLenti-sRNA-GFP lentiviral vector targeting the sequence 5'-CCACCTTATGTCTACAATCAAAAGAGCAT-3' of *Plac1* mRNA (cat #i034429, ABM, Vancouver, Canada) or the sequence 5'-CTGCACCCAAACCGAAGTCATAGCCACAC-3' of *Cxcl1* mRNA (cat # i042697, ABM); a scrambled sequence was used as a control. Lentivirus expression of *Cxcl1* utilized Lenti ORF clone *Cxcl1* (MR220966L1) from Origene and lenti vector CMV-m*Cxcl1*-IRES-mCherry (VB170524-1062) from VectorBuilder or the vector lacking *Cxcl1* as a control. HEK293T cells were co-transfected at 50% confluence with the lentiviral shRNA plasmid, psPAX2 packaging plasmid and the VSV-G/pMD2 envelope plasmid at a ratio of 2:1:0.1 using Fugene 6 (Promega). After 18 hr, medium was replaced with fresh growth medium, and after 24–48 hr, the virus-containing supernatant was collected, filtered through a 0.45 μ m filter, mixed with fresh cell culture medium at a ratio of 7:1, and added to EO771 cells with 8 μ g/ml polybrene. A lentivirus expressing a scrambled non-silencing control shRNA (shRNAmir, ABM) served as a negative control. Cells were selected for stable integration of the virus by incubation with 7.5 μ g/ml puromycin (Sigma-Aldrich Corp.) for 10 days. The efficiency of integration was monitored by GFP expression by the lentivirus. Cell lines 34T, 105T, 437T, MC and NeuT were described previously^{50,51}.

Animals. EO771 cells at an inoculum of 1×10^6 cells/0.1 ml were injected into the no. 4 mammary gland of C57BL/6 or SCID mice (Taconic), and tumor growth was monitored daily. *Cxcr2* antagonist SB225002 (Sigma-Aldrich) was dissolved in a diluent containing 8% DMSO, 10% PEG-400 and 1.75% Tween-20 in water at a concentration of 0.4 or 4.0 mg/ml, and administered i.p. Monday through Friday at a dose of 2 or 20 mg/kg, respectively^{52,53}. Other mouse mammary tumor cells lines tested for *Plac1* expression were 34T, 105T, 437T and MC^{40,51}. Animal studies were conducted under protocols approved by the Georgetown University Animal Care and Use Committee (protocol 2016-1143) in accordance with NIH guidelines for the ethical treatment of animals.

Cell growth and cytotoxicity assays. EO771 or MC cells were grown in 96-well plates at an initial density of 5,000 cells per well. The cytotoxicity of SB225002 was determined in EO771 cells by dissolving the drug in DMSO and diluting in medium to a final DMSO concentration of 0.001%. Cell density was determined after incubation for 24, 48 and 72 hr by sulforhodamine B staining and measuring optical density at 570 nm⁵⁴. Cytotoxicity assay data are shown in Supplementary Fig. 3.

Histopathology and immunohistochemistry (IHC). Mammary tumors were excised, and formalin-fixed, paraffin-embedded sections were prepared for H&E staining and IHC by the Tissue and Histopathology Shared Resource, LCCC. Antigen retrieval was carried out by incubation of tissue sections in 10 mM sodium citrate buffer (pH 6.0) for 20 min at a sub-boiling temperature in an electric steamer as previously described^{14,51,55}. Endogenous peroxidase activity was quenched with 3% hydrogen peroxide for 10 min, and incubated for 30 min with blocking solution (10% goat serum in Tris-buffered saline), followed by incubation overnight at 4 °C with the appropriate primary antibody diluted in blocking solution. Biotin-conjugated secondary antibodies were diluted in TBS containing 0.1% Tween-20 and incubated for 30 min at room temperature using the ABC Vectastain (Vector Laboratories) detection system and diaminobenzidine (Pierce), and slides were counterstained with Harris-modified hematoxylin (Thermo-Fisher, Inc.), dehydrated and mounted in PermOUNT (Thermo-Fisher, Inc.). Apoptosis was determined with the SignalStain Apoptosis IHC Detection kit for cleaved caspase-3 (Cell Signaling Technology). Antibodies and their dilutions for IHC and FACS are listed in Supplementary Table 1.

Fluorescence-Activated Cell Sorting (FACS). Tumor immune infiltrates were obtained by excising tumors, mincing them into small pieces and digestion with collagenase D (Roche) at a ratio of 15 ml collagenase solution per 2 g of tissue for 1 hr at 37 °C with shaking. The cell suspension was filtered through a 70 µm cell strainer (Falcon), washed, erythrocytes lysed and 1×10^6 cells were analyzed by FACS. Cells were stained using the Live/Dead Fixable Dead Cell Stain Kit (Invitrogen) and excluded from analysis, and non-specific binding was blocked with Fc antibody CD16/32 (Biolegend). Cells were first sorted for CD45 (macrophages, MDSC, Treg cells, NK cells and dendritic cells), CD45⁺CD3⁺ (T cells) or CD45⁺CD4⁺ (Treg cells). Cells were further sorted for: macrophages: F4/80⁺/MHCII⁺, MDSC: CD11b⁺/Gr-1⁺, dendritic cells: CD11c⁺/MHCII⁺, T cells: CD4⁺/CD8⁺, NK cells: CD45⁺/NK1.1⁺ and Treg cells: CD25⁺/Foxp3⁺. The fluorescent-conjugated monoclonal antibodies and their dilutions are listed in Supplementary Table 1. Cells were stained for Foxp3 after fixation in 1% paraformaldehyde and permeabilization (Permeabilization Buffer, eBioscience). Flow cytometry data was acquired by the Flow Cytometry & Cell Sorting Shared Resource, LCCC, with a BD LSRFortessa analyzer (BD Biosciences) and FCS Express 4 software (De Novo Software) to determine mean fluorescence intensity.

Gene microarray analysis. Microarray analysis was carried out as previously described^{39,51,55–57}. Briefly, tissue was snap-frozen in liquid nitrogen, pulverized in a mortar and pestle and RNA was extracted using an RNeasy Mini Kit (Qiagen) according to the manufacturer's protocol. RNA purity was assessed by the integrity of 18S and 28S rRNA using an Agilent microfluidic chip. Array analysis was carried out with cRNA prepared from equal amounts of RNA (1 µg) pooled from three replicates of cells per group. Biotin-labeled cRNA was fragmented at 94 °C for 35 min and hybridized overnight to an Affymetrix mouse 430A 2.0 GeneChip®, and scanned with an Agilent Gene Array scanner. Grid alignment and raw data generation used the Affymetrix GeneChip® Operating software 1.1. A noise value (Q) based on the variance of low-intensity probe cells was used to calculate a minimum threshold for each GeneChip. Samples were averaged and data refined by eliminating genes with signal intensities <300 in both comparison groups, and heat maps were generated from ≥ 3 -fold changes in gene expression normalized to control tissue using unsupervised hierarchical cluster analysis as previously described⁵⁸. Gene expression data for EO771 control, EO881/shPlac1 and EO771/shCxcl1 cells are included in Supplementary Tables 2 and 3, respectively. Gene expression data for mice treated with vehicle or 20 mg/kg SB25001 are included in Supplementary Table 4. Gene interaction analysis utilized Ariadne Pathway Studio version 9.1 (Supplementary Fig. 4). Data sets were deposited in the GEO public database under accession no. GSE78202.

Quantitative real-time polymerase chain reaction (qRT-PCR). Total RNA was extracted as described above, and RNA (1 µg) from each of 3 samples per group was reverse transcribed using the Omniscript RT kit (Qiagen) as previously described^{39,51,55–57}. PCR was performed in triplicate using an ABI-Prism 7700 (Applied Biosystems, Foster City, CA) with SYBRGreen I detection (Qiagen) according to the manufacturer's protocol. Amplification using the appropriate primers (Supplementary Table 5) was confirmed by ethidium bromide staining of the PCR products on an agarose gel. The expression of each target gene was normalized to GAPDH and is presented as the ratio of the target gene to GAPDH expression calculated using the formula, $2^{-\Delta Ct}$, where $\Delta Ct = Ct_{\text{Target}} - Ct_{18s}$ ³⁹.

Statistical analysis. Statistical significance of means \pm S.D. were evaluated using the two-tailed Student's t test at a significance of $P < 0.05$. Differences in tumor growth *in vivo* were determined by the unpaired two-tailed Student's t test at a significance of $P < 0.05$.

References

1. Fant, M., Farina, A., Nagaraja, R. & Schlessinger, D. PLAC1 (Placenta-specific 1): a novel, X-linked gene with roles in reproductive and cancer biology. *Prenat. Diagn.* **30**, 497–502 (2011).
2. Silva, W. A. Jr *et al.* PLAC1, a trophoblast-specific cell surface protein, is expressed in a range of human tumors and elicits spontaneous antibody responses. *Cancer immunity* **7**, 18 (2007).
3. Old, L. J. Cancer is a somatic cell pregnancy. *Cancer immunity* **7**, 19 (2007).
4. Grigoriadis, A. *et al.* CT-X antigen expression in human breast cancer. *Proc. Natl. Acad. Sci. USA* **106**, 13493–13498, <https://doi.org/10.1073/pnas.0906840106> (2009).
5. Koslowski, M. *et al.* A placenta-specific gene ectopically activated in many human cancers is essentially involved in malignant cell processes. *Cancer Res.* **67**, 9528–9534 (2007).
6. Wang, X., Baddoo, M. C. & Yin, Q. The placental specific gene, PLAC1, is induced by the Epstein-Barr virus and is expressed in human tumor cells. *Virology journal* **11**, 107, <https://doi.org/10.1186/1743-422X-11-107> (2014).
7. Devor, E. J. & Leslie, K. K. The oncoplacental gene placenta-specific protein 1 is highly expressed in endometrial tumors and cell lines. *Obstetrics and gynecology international* **2013**, 807849, <https://doi.org/10.1155/2013/807849> (2013).

8. Cheung, H. W. *et al.* Systematic investigation of genetic vulnerabilities across cancer cell lines reveals lineage-specific dependencies in ovarian cancer. *Proc. Natl. Acad. Sci. USA* **108**, 12372–12377, <https://doi.org/10.1073/pnas.1109363108> (2011).
9. Dong, X. Y. *et al.* Plac1 is a tumor-specific antigen capable of eliciting spontaneous antibody responses in human cancer patients. *Int. J. Cancer* **122**, 2038–2043 (2008).
10. Liu, F. *et al.* Identification of two new HLA-A*0201-restricted cytotoxic T lymphocyte epitopes from colorectal carcinoma-associated antigen PLAC1/CP1. *J. Gastroenterol.* **49**, 419–426, <https://doi.org/10.1007/s00535-013-0811-4> (2014).
11. Liu, F. F. *et al.* The specific immune response to tumor antigen CP1 and its correlation with improved survival in colon cancer patients. *Gastroenterology* **134**, 998–1006 (2008).
12. Otsubo, T. *et al.* MicroRNA-126 Inhibits SOX2 Expression and Contributes to Gastric Carcinogenesis. *PLoS one* **6**, e16617 (2011).
13. Ghods, R. *et al.* High placenta-specific 1/low prostate-specific antigen expression pattern in high-grade prostate adenocarcinoma. *Cancer Immunol. Immunother.* **63**, 1319–1327, <https://doi.org/10.1007/s00262-014-1594-z> (2014).
14. Yuan, H. *et al.* PPARdelta induces estrogen receptor-positive mammary neoplasia through an inflammatory and metabolic phenotype linked to mTOR activation. *Cancer Res.* **73**, 4349–4361, <https://doi.org/10.1158/0008-5472.CAN-13-0322> (2013).
15. Adhikary, T. *et al.* Genomewide analyses define different modes of transcriptional regulation by peroxisome proliferator-activated receptor-beta/delta (PPARbeta/delta). *PLoS one* **6**, e16344, <https://doi.org/10.1371/journal.pone.0016344> (2011).
16. Torres-Arzuayus, M. I. *et al.* High tumor incidence and activation of the PI3K/AKT pathway in transgenic mice define AIB1 as an oncogene. *Cancer cell* **6**, 263–274 (2004).
17. Torres-Arzuayus, M. I., Zhao, J., Bronson, R. & Brown, M. Estrogen-dependent and estrogen-independent mechanisms contribute to AIB1-mediated tumor formation. *Cancer Res.* **70**, 4102–4111, <https://doi.org/10.1158/0008-5472.CAN-09-4080> (2010).
18. Koslowski, M. *et al.* Selective activation of trophoblast-specific PLAC1 in breast cancer by CCAAT/enhancer-binding protein beta (C/EBPbeta) isoform 2. *J. Biol. Chem.* **284**, 28607–28615 (2009).
19. Wagner, M. *et al.* NCOA3 is a selective co-activator of estrogen receptor alpha-mediated transactivation of PLAC1 in MCF-7 breast cancer cells. *BMC cancer* **13**, 570, <https://doi.org/10.1186/1471-2407-13-570> (2013).
20. Anzick, S. L. *et al.* AIB1, a steroid receptor coactivator amplified in breast and ovarian cancer. *Science* **277**, 965–968 (1997).
21. Liao, L. *et al.* Molecular structure and biological function of the cancer-amplified nuclear receptor coactivator SRC-3/AIB1. *J. Steroid Biochem. Mol. Biol.* **83**, 3–14 (2002).
22. Grimm, S. L. & Rosen, J. M. The role of C/EBPbeta in mammary gland development and breast cancer. *J. Mammary Gland Biol. Neoplasia* **8**, 191–204 (2003).
23. Lunghi, L., Ferretti, M. E., Medici, S., Biondi, C. & Vesce, F. Control of human trophoblast function. *Reproductive biology and endocrinology: RB&E* **5**, 6, <https://doi.org/10.1186/1477-7827-5-6> (2007).
24. Clark, D. A., Chaput, A. & Tutton, D. Active suppression of host-vs-graft reaction in pregnant mice. VII. Spontaneous abortion of allogeneic CBA/J × DBA/2 fetuses in the uterus of CBA/J mice correlates with deficient non-T suppressor cell activity. *J. Immunol.* **136**, 1668–1675 (1986).
25. Topalian, S. L., Drake, C. G. & Pardoll, D. M. Immune checkpoint blockade: a common denominator approach to cancer therapy. *Cancer cell* **27**, 450–461, <https://doi.org/10.1016/j.ccell.2015.03.001> (2015).
26. Li, B. *et al.* Comprehensive analyses of tumor immunity: implications for cancer immunotherapy. *Genome biology* **17**, 174, <https://doi.org/10.1186/s13059-016-1028-7> (2016).
27. Chen, Y., Moradin, A., Schlessinger, D. & Nagaraja, R. RXRalpha and LXR activate two promoters in placenta- and tumor-specific expression of PLAC1. *Placenta* **32**, 877–884, <https://doi.org/10.1016/j.placenta.2011.08.011> (2011).
28. Cocchia, M. *et al.* PLAC1, an Xq26 gene with placenta-specific expression. *Genomics* **68**, 305–312 (2000).
29. Bezbradica, J. S. & Medzhitov, R. Integration of cytokine and heterologous receptor signaling pathways. *Nature immunology* **10**, 333–339, <https://doi.org/10.1038/ni.1713> (2009).
30. Acharyya, S. *et al.* A CXCL1 paracrine network links cancer chemoresistance and metastasis. *Cell* **150**, 165–178, <https://doi.org/10.1016/j.cell.2012.04.042> (2012).
31. Di Mitri, D. *et al.* Tumour-infiltrating Gr-1+ myeloid cells antagonize senescence in cancer. *Nature* **515**, 134–137, <https://doi.org/10.1038/nature13638> (2014).
32. Zou, A. *et al.* Elevated CXCL1 expression in breast cancer stroma predicts poor prognosis and is inversely associated with expression of TGF-beta signaling proteins. *BMC cancer* **14**, 781, <https://doi.org/10.1186/1471-2407-14-781> (2014).
33. Finak, G. *et al.* Stromal gene expression predicts clinical outcome in breast cancer. *Nat. Med.* **14**, 518–527, <https://doi.org/10.1038/nm1764> (2008).
34. Bieche, I. *et al.* CXC chemokines located in the 4q21 region are up-regulated in breast cancer. *Endocrine-related cancer* **14**, 1039–1052, <https://doi.org/10.1677/erc.1.01301> (2007).
35. Harbeck, N., Schmitt, M., Paepke, S., Allgayer, H. & Kates, R. E. Tumor-associated proteolytic factors uPA and PAI-1: critical appraisal of their clinical relevance in breast cancer and their integration into decision-support algorithms. *Crit. Rev. Clin. Lab. Sci.* **44**, 179–201, <https://doi.org/10.1080/10408360601040970> (2007).
36. Lala, P. K. & Chakraborty, C. Factors regulating trophoblast migration and invasiveness: possible derangements contributing to pre-eclampsia and fetal injury. *Placenta* **24**, 575–587 (2003).
37. Grange, C., Lanzardo, S., Cavallo, F., Camussi, G. & Bussolati, B. Sca-1 identifies the tumor-initiating cells in mammary tumors of BALB-neuT transgenic mice. *Neoplasia* **10**, 1433–1443 (2008).
38. Liu, J. C., Deng, T., Lehal, R. S., Kim, J. & Zacksenhaus, E. Identification of tumorsphere- and tumor-initiating cells in HER2/Neu-induced mammary tumors. *Cancer Res.* **67**, 8671–8681 (2007).
39. Upadhyay, G. *et al.* Stem cell antigen-1 enhances tumorigenicity by disruption of growth differentiation factor-10 (GDF10)-dependent TGF-beta signaling. *Proc. Natl. Acad. Sci. USA* **108**, 7820–7825, <https://doi.org/10.1073/pnas.1103441108> (2011).
40. Yuan, H., Upadhyay, G., Yin, Y., Kopelovich, L. & Glazer, R. I. Stem cell antigen-1 deficiency enhances the chemopreventive effect of peroxisome proliferator-activated receptor{gamma} activation. *Cancer prevention research* **5**, 51–60 (2012).
41. Biswas, S. K. & Mantovani, A. Macrophage plasticity and interaction with lymphocyte subsets: cancer as a paradigm. *Nature immunology* **11**, 889–896, <https://doi.org/10.1038/ni.1937> (2010).
42. DeNardo, D. G. *et al.* Leukocyte complexity predicts breast cancer survival and functionally regulates response to chemotherapy. *Cancer discovery* **1**, 54–67, <https://doi.org/10.1158/2159-8274.CD-10-0028> (2011).
43. Hendriks-Balk, M. C. *et al.* Sphingosine-1-phosphate regulates RGS2 and RGS16 mRNA expression in vascular smooth muscle cells. *Eur. J. Pharmacol.* **606**, 25–31, <https://doi.org/10.1016/j.ejphar.2009.01.018> (2009).
44. Jackman S. K. X. & Fant M. Plac1 (Placenta-specific 1) Is Essential for Normal Placental and Embryonic Development. *Mol. Reprod. Dev.* in press (2012).
45. Stadtmann, A. & Zarbock, A. CXCR2: From Bench to Bedside. *Frontiers in immunology* **3**, 263, <https://doi.org/10.3389/fimmu.2012.00263> (2012).
46. Horuk, R. Chemokine receptor antagonists: overcoming developmental hurdles. *Nature reviews. Drug discovery* **8**, 23–33, <https://doi.org/10.1038/nrd2734> (2009).
47. Jamieson, T. *et al.* Inhibition of CXCR2 profoundly suppresses inflammation-driven and spontaneous tumorigenesis. *J. Clin. Invest.* **122**, 3127–3144, <https://doi.org/10.1172/JCI61067> (2012).
48. Highfill, S. L. *et al.* Disruption of CXCR2-mediated MDSC tumor trafficking enhances anti-PD1 efficacy. *Science translational medicine* **6**, 237ra267, <https://doi.org/10.1126/scitranslmed.3007974> (2014).

49. Dunham, L. J. & Stewart, H. L. A survey of transplantable and transmissible animal tumors. *J. Natl. Cancer Inst.* **13**, 1299–1377 (1953).
50. Lindsay, J. *et al.* ErbB2 induces Notch1 activity and function in breast cancer cells. *Clinical and translational science* **1**, 107–115, <https://doi.org/10.1111/j.1752-8062.2008.00041.x> (2008).
51. Yin, Y., Yuan, H., Zeng, X., Kopelovich, L. & Glazer, R. I. Inhibition of peroxisome proliferator-activated receptor gamma increases estrogen receptor-dependent tumor specification. *Cancer Res.* **69**, 687–694, <https://doi.org/10.1158/0008-5472.CAN-08-2446> (2009).
52. de Vasconcellos, J. F. *et al.* SB225002 Induces Cell Death and Cell Cycle Arrest in Acute Lymphoblastic Leukemia Cells through the Activation of GLIPR1. *PLoS one* **10**, e0134783, <https://doi.org/10.1371/journal.pone.0134783> (2015).
53. Ijichi, H. *et al.* Inhibiting Cxcr2 disrupts tumor-stromal interactions and improves survival in a mouse model of pancreatic ductal adenocarcinoma. *J. Clin. Invest.* **121**, 4106–4117, <https://doi.org/10.1172/JCI42754> (2011).
54. Skehan, P. *et al.* New colorimetric cytotoxicity assay for anticancer-drug screening. *J. Natl. Cancer Inst.* **82**, 1107–1112 (1990).
55. Yin, Y. *et al.* Peroxisome proliferator-activated receptor delta and gamma agonists differentially alter tumor differentiation and progression during mammary carcinogenesis. *Cancer Res.* **65**, 3950–3957 (2005).
56. Pollock, C. B. *et al.* PPARdelta activation acts cooperatively with 3-phosphoinositide-dependent protein kinase-1 to enhance mammary tumorigenesis. *PLoS one* **6**, e16215, <https://doi.org/10.1371/journal.pone.0016215> (2011).
57. Yin, Y. *et al.* Characterization of medroxyprogesterone and DMBA-induced multilineage mammary tumors by gene expression profiling. *Mol. Carcinog.* **44**, 42–50, <https://doi.org/10.1002/mc.20119> (2005).
58. Herschkowitz, J. I. *et al.* Identification of conserved gene expression features between murine mammary carcinoma models and human breast tumors. *Genome biology* **8**, R76, <https://doi.org/10.1186/gb-2007-8-5-r76> (2007).

Acknowledgements

This work was supported by grants from the Nina Hyde Foundation, the Avon Foundation for Women, contract INO1 CN43302-WA19 from the National Cancer Institute, NIH, and award 1P30 CA051008 from the National Cancer Institute, NIH, to the Lombardi Comprehensive Cancer Center. This investigation was conducted using the Animal Research, Genomics and Epigenomics, Tissue and Histology and Microscopy and Imaging Shared Resources of the LCCC, and by an animal facilities construction grant from the NIH.

Author Contributions

R.I.G. conceived of the hypothesis. R.I.G., H.Y., L.M.W. and Y.T. designed the experiments. H.Y., X.W., C.S., L.J., J.L., J.H., N.V., V.D., and S.W., A.Z. performed the experiments. R.I.G., H.Y., L.J. and J.L. analyzed and interpreted the data. R.I.G. and H.Y. wrote the manuscript.

Additional Information

Supplementary information accompanies this paper at <https://doi.org/10.1038/s41598-018-24022-w>.

Competing Interests: The authors declare no competing interests.

Publisher's note: Springer Nature remains neutral with regard to jurisdictional claims in published maps and institutional affiliations.



Open Access This article is licensed under a Creative Commons Attribution 4.0 International License, which permits use, sharing, adaptation, distribution and reproduction in any medium or format, as long as you give appropriate credit to the original author(s) and the source, provide a link to the Creative Commons license, and indicate if changes were made. The images or other third party material in this article are included in the article's Creative Commons license, unless indicated otherwise in a credit line to the material. If material is not included in the article's Creative Commons license and your intended use is not permitted by statutory regulation or exceeds the permitted use, you will need to obtain permission directly from the copyright holder. To view a copy of this license, visit <http://creativecommons.org/licenses/by/4.0/>.

© The Author(s) 2018

Plac1 Is a Key Regulator of the Inflammatory Response and Immune Tolerance In Mammary Tumorigenesis

Hongyan Yuan, Xiaoyi Wang, Chunmei Shi, Lu Jin, Jianxia Hu, Alston Zhang, James Li, Nairuthya Vijayendra, Venkata Doodala, Spencer Weiss, Yong Tang, Louis M. Weiner and Robert I. Glazer.

Supplementary Data

Supplementary Figure 1. EO771/sh490/sh187 Plac1 tumor growth

Supplementary Figure 2. SB225002 cytotoxicity assay

Supplementary Figure 3. MC/Plac1 cells

Supplementary Figure 4. Immune signaling pathways

Supplementary Table 1. Antibodies for IHC and FACS

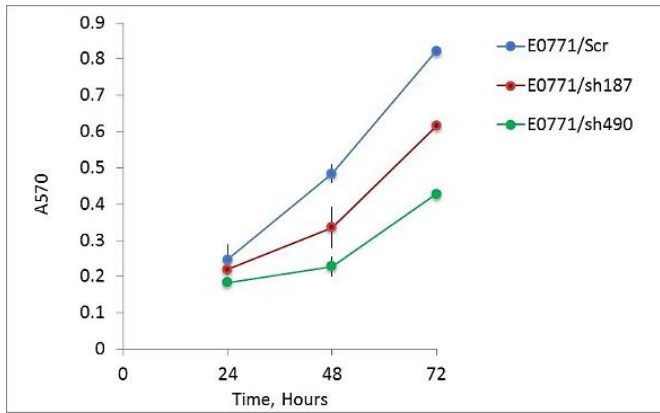
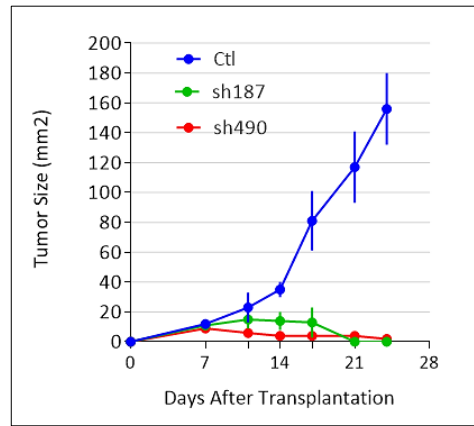
Supplementary Table 2. Gene expression in EO771/shPlac1 cells

Supplementary Table 3. Gene expression in EO771/shCxcl1 cells

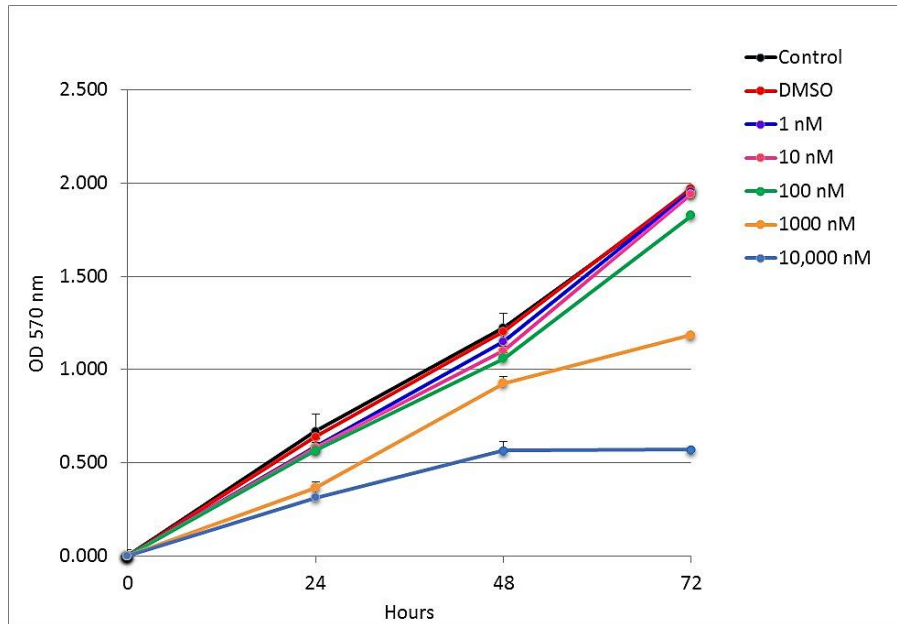
Supplementary Table 4. Gene expression in EO771 tumors+SB25002 treatment

Supplementary Table 5. Gene expression for MC/Plac1 cells

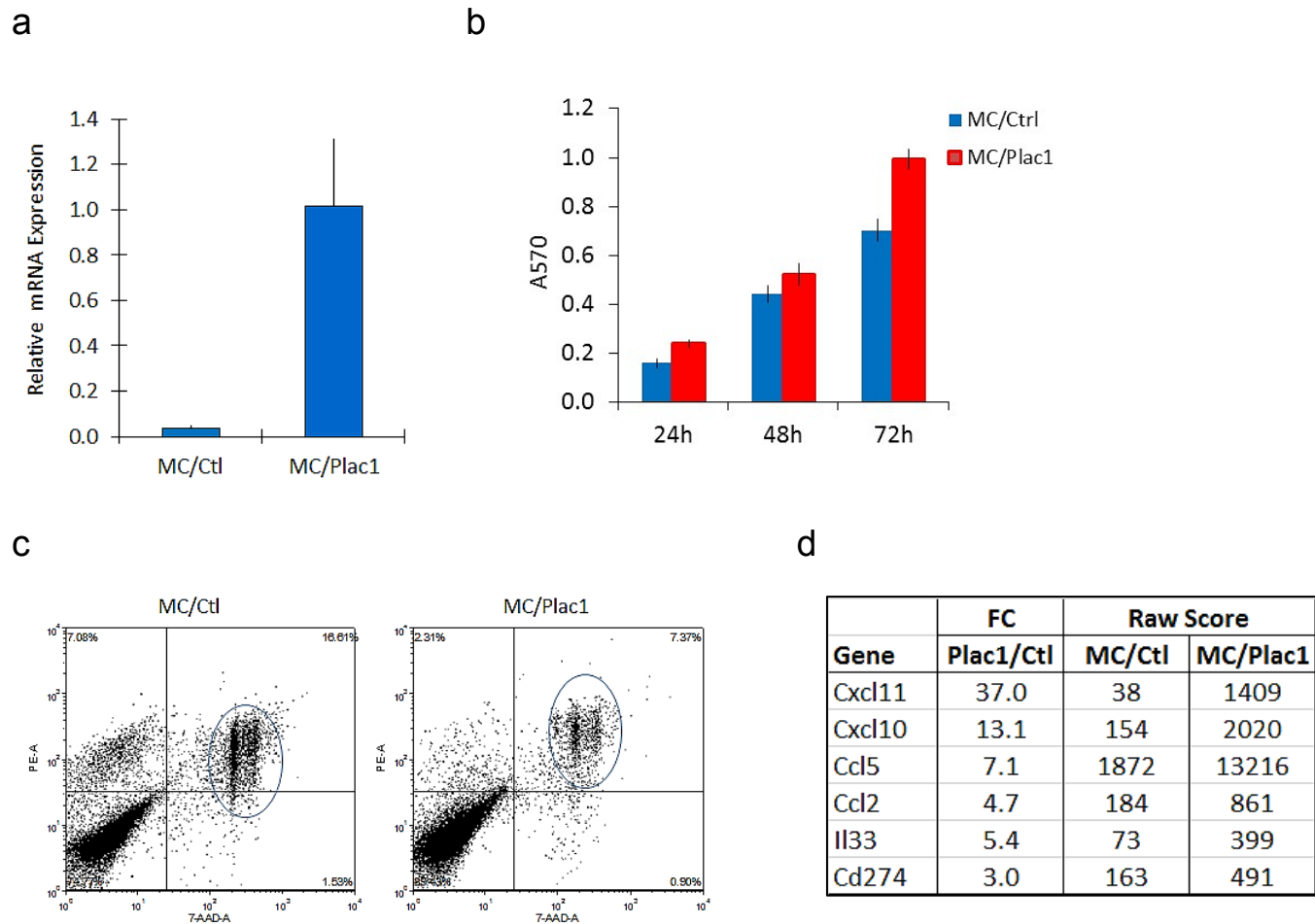
Supplementary Table 6. List of primers for qRT-PCR analysis.

a**b**

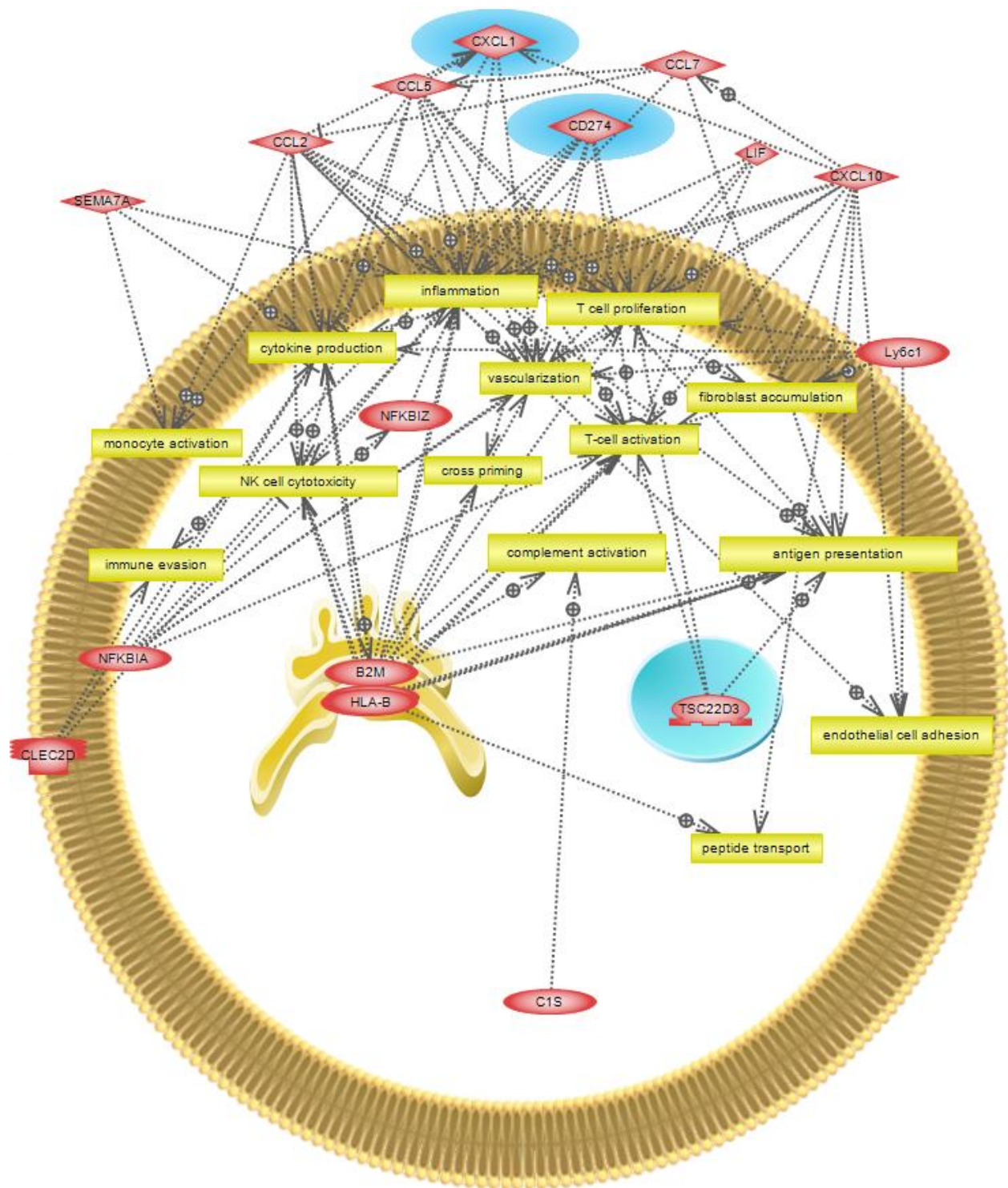
Supplementary Figure 1. Growth of EO771/Scr, EO771/sh187 and EO771/sh490 cells, and the effect of Cxcl1 co-expression in EO771/sh490 cells. (a) EO771/Scr, EO771/sh187 and EO771/sh490 cells were grown as monolayers and cell density determined by sulforhodamine B staining and measuring the absorbance at 570 nm. Shown is the mean±S.D. of triplicate determinations. The growth of EO771/sh490 cells differed significantly ($P<0.001$) from EO771/Scr cells at 24-72 hr using the two-sided Student's t test. (b) C57BL/6 mice at five weeks of age, were inoculated in the mammary gland with 1×10^6 cells, and tumor size determined by caliper measurement in two dimensions. The growth of EO771/sh187 or EO771/sh490 cells differed significantly from EO771/Scr ($P<0.01$) by the unpaired Student's t test. Shown is the mean±SD, N=6 per group.



Supplementary Figure 2. In vitro cytotoxicity of SB225002 to EO771 cells. EO771 cells were grown in 96-well plates at an initial density of 5,000 cells per well, and treated with 0.001% DMSO or SB225002. Cell density was determined after 24, 48 and 72 hr by sulforhodamine B staining and measuring absorbance at 570 nm. Indicated is the final concentration (nM) of SB225002. Shown is the mean \pm SD of triplicate determinations.



Supplementary Figure 3. Overexpression of Plac1 in MC mammary tumor cells. (a) qRT-PCR analysis of MC/Plac1 cells transfected with a vector expressing murine Plac1 and selected in G-418. MC/Plac1 cells expressed significantly greater levels of Plac1 than control MC/Ctl cells by the two-sided Student's t test ($P < 0.001$, $N = 3$). (b) MC/Plac1 cells were grown in a 96-well plate at an initial density of 5,000 cells per well for 24-72 hr, and cell density determined by sulforhodamine B staining and measuring absorbance at 570 nm. Shown is the mean \pm SD of triplicate determinations. (c) Analysis of apoptosis in MC/Plac1 cells by fluorescence of 7-aminoactinomycin D as a measure of cell viability. The scatter determined by FACS is *circled* and is a measure of late apoptosis, which decreased from 16.6% in MC/Ctl cells to 7.3% in MC/Plac1 cells. (d) Table of chemokine and immune-related gene expression in MC/Ctl and MC/Plac1 cells as determined by Affymetrix gene expression profiling (see Supplementary Table 5 for full list).



Supplementary Figure 4. Schematic of immune signaling by Plac1 in EO771 cells. Based on data in Table 1, EO771 cells overexpress several chemokines and immune factors, which regulate inflammation, cytokine production, fibroblast activation, antigen presentation, and monocyte and T cell activation. Plac1 maintained high CXCL1 expression, a chemokine that activates CXCR2 on MDSC, whereas, CD274/ PD-L1 expressed by MDSC and tumor cells activates Treg cells; both pathways contribute to immune tolerance. Inhibition of CXCR2 with an antagonist and treatment with a PD-L1 mAb counteracts in part activation of a tolerogenic tumor microenvironment.

Supplementary Table 1. Antibodies for IHC and FACS.

	Catalog #	Source	Dilution	
			IHC	FACS
anti-Plac1	sc-365919	Santa Cruz	400	
anti-PD-L1	17952-I-AP	Proteintech	200	
anti-Cxcl1	sc-1374	Santa Cruz	120	
anti-CD8a	14-0808-82	eBioscience	40	
anti-SMA	sc130617	Santa Cruz	100	
anti-Ki67	CRM325	Biocare	50	
anti-CD31	ab56299	abcam	100	
anti-Foxp3	14-5773-82	eBioscience	50	
CD16/32	101301	Biolegend		100
FITC anti-mouse CD4	100509	Biolegend		200
PE/Cy7 anti-mouse CD8a	100721	Biolegend		40
APC anti-mouse CD3 epsilon	100311	Biolegend		100
APC anti-mouse CD25	102011	Biolegend		400
PE anti-mouse CD80	104707	Biolegend		400
PE anti-mouse CD86	105007	Biolegend		125
APC anti-mouse F4/80	123115	Biolegend		80
APC/Cy7 anti-mouse CD45	103115	Biolegend		80
PE anti-mouse NK1.1	108707	Biolegend		80
APC anti-mouse CD11c	117309	Biolegend		80
APC anti-mouse/human CD11b	101211	Biolegend		80
PE anti-mouse Foxp3	12-4771-80	eBioscience		80
PE/Cy7 anti-mouse Ly6g/Ly6c (Gr-1)	108415	Biolegend		200

Supplementary Table 2. Gene expression in EO771/shPlac1 cells. Shown are genes with ≥ 3 -fold change in expression and a raw score ≥ 300 in EO771/shPlac1 or EO771/Scr cells.

Function	log2		Raw Score		FC	Gene Name
	Scr	shPlac1	Scr	shPlac1	shPlac1/Scr	
Adhesion/ECM						
Pkp2	6.63	8.27	99	308	3.1	plakophilin 2
P4ha2	11.33	9.66	2567	811	-3.1	prolyl 4-hydroxylase, alpha polypeptide II
Sdc1	11.58	9.88	3064	939	-3.2	syndecan 1
Col18a1	10.35	8.42	1301	343	-3.7	collagen, type XVIII, alpha 1
Apoptosis						
Birc5	8.74	10.53	427	1478	3.5	baculoviral IAP repeat containing 5; Survivin
Ebag9	6.75	8.43	107	345	3.2	estrogen receptor binding site associated, antigen, 9
CD82	10.83	8.96	1823	498	-3.7	Kangai 1 (suppression of tumorigenicity 6, prostate;
Trp53inp1	8.30	6.34	314	81	-3.8	tumor protein p53 inducible nuclear protein 1
Differentiation						
Pter	6.83	8.62	114	394	3.5	phosphotriesterase related
Krt8	10.83	12.42	1817	5489	3.0	keratin 8
Gdf15	9.71	8.12	840	279	-3.3	growth differentiation factor 15
DNA Repair						
Fign1	7.05	9.56	132	757	5.7	fidgetin-like 1
Rad51	6.51	8.75	91	431	4.7	RAD51 recombinase
Fen1	6.89	9.08	119	540	4.6	flap structure-specific endonuclease 1
Rad51ap1	6.37	8.51	83	365	4.5	RAD51 associated protein 1
Ercc6l	6.71	8.83	105	456	4.4	excision repair cross-complementation group 6-like
Rad54l	6.24	8.25	75	305	4.1	RAD54-like (S. cerevisiae)
Ddit3	10.19	8.16	1166	286	-4.0	DNA-damage-inducible transcript 3
Gadd45b	10.55	7.31	1499	159	-12.5	growth arrest and DNA-damage-inducible, beta
DNA Synthesis						
Mki67	7.10	9.99	137	1020	7.4	marker of proliferation Ki-67
Tyms	5.99	8.56	64	378	5.9	thymidylate synthetase
Mcm5	6.42	8.87	86	467	5.4	minichromosome maintenance complex component 5
Cdc6	6.00	8.36	64	328	5.1	cell division cycle 6
Rrm2	9.22	11.28	596	2487	4.4	ribonucleotide reductase M2
Rrm1	8.32	10.34	320	1296	4.1	ribonucleotide reductase M1
Pola1	7.15	9.10	142	549	3.9	polymerase (DNA directed), alpha 1, catalytic subunit
Mcm3	8.10	9.88	274	942	3.5	minichromosome maintenance complex component 3
Mcm4	8.11	9.90	276	955	3.5	minichromosome maintenance complex component 4
Prim1	7.73	9.47	212	709	3.4	primase, DNA, polypeptide 1 (49kDa)
Nasp	8.10	9.73	275	850	3.1	nuclear autoantigenic sperm protein (histone-binding)
Mcm7	8.85	10.45	462	1399	3.0	minichromosome maintenance complex component 7
Smardc1	7.83	9.43	228	690	3.0	SWI/SNF related, matrix associated, actin dependent regulator of chromatin, subfamily b, member 1
Immune/Inflammation						
Tapbp	11.71	10.11	3356	1102	-3.0	TAP binding protein (tapasin)
CD274	8.24	6.50	302	91	-3.3	programmed cell death 1 ligand 1
Cxcl10	8.84	7.02	459	130	-3.6	chemokine (C-X-C motif) ligand 10
Sema7a	8.74	6.93	426	122	-3.6	semaphorin 7A, GPI membrane anchor (John Milton Hagen blood group)
Ifi44	9.35	7.50	652	181	-3.6	interferon-induced protein 44
Ly6c1	10.23	8.36	1198	329	-3.7	lymphocyte antigen 6 complex, locus C
Clec2d	8.51	6.62	366	99	-3.7	C-type lectin domain family 2, member D
Nfkbi2	9.22	7.17	596	144	-4.4	nuclear factor of kappa light polypeptide gene enhancer in B-cells inhibitor, zeta
Ly6a	12.27	10.18	4937	1160	-4.3	lymphocyte antigen 6 complex, locus A, stem cell antigen-1
H2-K1	11.02	8.90	2069	478	-4.5	major histocompatibility complex, class I, K
Tsc22d3	11.15	8.90	2265	478	-4.8	TSC22 domain family, member 3
Ccl5	11.90	9.61	3812	784	-4.8	chemokine (C-C motif) ligand 5
H2-D1	11.20	8.88	2353	471	-5.0	major histocompatibility complex, class I, D
B2m	8.58	6.16	383	72	-5.3	beta-2-microglobulin
Nfkbia	12.08	9.02	4330	517	-7.1	nuclear factor of kappa light polypeptide gene enhancer in B-cells inhibitor, alpha
C1s	9.84	7.00	918	128	-7.1	complement component 1, s subcomponent
Lif	9.37	6.32	664	80	-8.3	leukemia inhibitory factor
Mndal	10.63	7.53	1585	185	-8.3	myeloid cell nuclear differentiation antigen
Ccl2	11.83	8.25	3640	305	-11.9	chemokine (C-C motif) ligand 2
CD68	9.86	5.78	929	55	-16.9	scavenger receptor class D, member 1
Ccl7	11.48	7.25	2854	153	-18.5	chemokine (C-C motif) ligand 7
Cxcl1	12.78	6.73	7054	106	-66.7	chemokine (C-X-C motif) ligand 1 (melanoma growth stimulating activity, alpha)
Invasion/Motility						
Diap3	5.59	8.59	48	386	9.1	diaphanous-related formin 3
Hmmr	7.51	9.33	182	644	3.5	hyaluronan-mediated motility receptor (RHAMM)
Racgap1	8.47	10.21	355	1184	3.3	Rac GTPase activating protein 1
Serpine1	10.98	9.35	2021	651	-3.1	serpin peptidase inhibitor, clade E (nexin, plasminogen activator inhibitor type 1), member 1
Ntn1	9.52	7.84	736	229	-3.2	netrin 1
Serpinf1	11.60	9.75	3097	860	-3.4	serpin peptidase inhibitor, clade F (alpha-2 antiplasmin, pigment epithelium derived factor), member 1
Ctsh	10.92	8.47	1931	354	-5.6	cathepsin H
Plau	9.34	6.31	646	80	-7.1	plasminogen activator, urokinase
Metabolism						
Pdss1	6.40	8.33	84	322	3.8	prenyl (decaprenyl) diphosphate synthase, subunit 1
Mgat2	7.70	9.33	208	643	3.1	mannosyl (alpha-1,6-)-glycoprotein beta-1,2-N-acetylglucosaminyltransferase
Sephs2	7.93	9.52	244	733	3.0	selenophosphate synthetase 2
Npc2	13.22	11.54	9553	2987	-3.2	Niemann-Pick disease, type C2
Idua	8.35	6.65	327	100	-3.2	iduronidase, alpha-L-
ND5	11.77	9.98	3486	1008	-3.4	mitochondrially encoded NADH dehydrogenase 5
Lipg	8.32	6.54	320	93	-3.6	lipase, endothelial
Ip6k1	9.86	7.72	932	211	-4.3	inositol hexakisphosphate kinase 1
St3gal1	8.53	6.33	370	80	-4.5	ST3 beta-galactoside alpha-2,3-sialyltransferase 1
Dnpep	8.79	6.46	444	88	-5.0	aspartyl aminopeptidase
Fabp4	10.76	7.33	1734	161	-11.4	fatty acid binding protein 4, adipocyte

Mitosis						
Melk	6.62	8.96	98	498	5.1	maternal embryonic leucine zipper kinase
Nuf2	6.74	9.05	107	529	5.0	NUF2, NDC80 kinetochore complex component
Cenpf	7.87	10.14	233	1126	4.8	centromere protein F, 350/400kDa
H1f0	8.62	10.75	392	1726	4.6	H1 histone family, member 0
Kif22	7.69	9.83	207	910	4.4	kinesin family member 22
Ccnb1	7.44	9.59	174	771	4.2	cyclin B1
Ndc80	6.37	8.43	83	345	4.2	NDC80 kinetochore complex component
Kif2c	7.23	9.26	150	613	4.1	kinesin family member 2C
Aspm	7.42	9.45	171	699	4.1	asp (abnormal spindle) homolog, microcephaly associated (Drosophila)
Ccna2	9.00	10.92	512	1941	3.8	cyclin A2
Ect2	8.08	10.01	270	1030	3.8	epithelial cell transforming 2
Ska1	6.72	8.63	106	396	3.7	spindle and kinetochore associated complex subunit 1
Spag5	6.65	8.42	100	342	3.5	sperm associated antigen 5
Cdca5	7.77	9.50	219	724	3.4	cell division cycle associated 5
Cenpt	6.81	8.55	112	376	3.4	centromere protein T
Nek2	7.03	8.76	130	434	3.3	NIMA-related kinase 2
Sgo1	7.74	9.47	214	710	3.3	shugoshin-like 1 (S. pombe)
Spc25	7.44	9.18	174	582	3.3	SPC25, NDC80 kinetochore complex component
Tacc3	7.88	9.59	236	772	3.3	transforming, acidic coiled-coil containing protein 3
Ncapd2	8.00	9.71	256	836	3.3	non-SMC condensin I complex, subunit D2
Ncapg	7.14	8.87	141	466	3.3	non-SMC condensin I complex, subunit G
Ncaph	7.99	9.58	255	766	3.2	non-SMC condensin I complex, subunit H
Aurka	8.74	10.37	428	1322	3.1	aurora kinase A
Tubb2a	7.48	9.10	178	550	3.1	tubulin, beta 2A class IIa
Cdc20	10.38	11.99	1333	4063	3.1	cell division cycle 20
Ndrp4	10.82	9.14	1808	564	-3.2	NDRG family member 4
Plk2	9.70	7.88	830	236	-3.6	polo-like kinase 2
Pafah1b1	8.89	7.01	474	129	-3.7	platelet-activating factor acetylhydrolase 1b, regulatory subunit 1 (45kDa)
Zwint	9.11	6.72	553	106	-5.3	ZW10 interacting kinetochore protein
Protein Trafficking/Degradation						
Diap2	5.59	8.59	48	386	8.0	diaphanous-related formin 2
Tubb4b	10.34	12.40	1299	5409	4.2	tubulin, beta 4B class IVb
Dnajc9	6.76	8.78	109	440	4.1	DnaJ (Hsp40) homolog, subfamily C, member 9
Uhrf1	7.38	9.22	167	598	3.6	ubiquitin-like with PHD and ring finger domains 1
Hspa4	8.20	9.98	294	1013	3.4	heat shock 70kDa protein 4
Ide	7.85	9.54	231	744	3.2	insulin-degrading enzyme
Fbnp4	8.37	6.78	330	110	-3.0	formin binding protein 4
Mapk8ip3	8.32	6.73	319	106	-3.0	mitogen-activated protein kinase 8 interacting protein 3
Trim30a	8.45	6.81	349	112	-3.1	tripartite motif containing 30
Gramd1a	10.03	8.39	1048	335	-3.1	GRAM domain containing 1A
Hspa5	13.38	11.63	10689	3170	-3.3	heat shock 70kDa protein 5 (glucose-regulated protein, 78kDa)
Calr	11.78	10.01	3517	1031	-3.4	calreticulin
Rcn3	11.45	9.61	2801	780	-3.6	reticulocalbin 3, EF-hand calcium binding domain
Vcp	8.26	6.36	308	82	-3.7	valosin containing protein
Srpb	9.14	7.18	564	145	-3.8	signal recognition particle receptor, B subunit
Rab14	8.39	6.38	336	83	-4.0	RAB14, member RAS oncogene family
Tmed3	11.31	9.24	2534	604	-4.2	transmembrane emp24 protein transport domain containing 3
Arih2	9.46	7.40	707	169	-4.2	ariadne RBR E3 ubiquitin protein ligase 2
Hspa1b	8.91	6.73	481	106	-4.3	heat shock 70kDa protein 1B
Fkbp7	9.45	7.34	700	162	-4.3	FK506 binding protein 7
Zfand2a	10.49	8.33	1438	321	-4.5	zinc finger, AN1-type domain 2A
Arl4d	10.49	8.33	1438	321	-5.0	ADP-ribosylation factor-like 4D
Dnajb6	9.54	7.19	746	146	-5.3	DnaJ (Hsp40) homolog, subfamily B, member 6
Cryab	10.39	7.84	1340	229	-5.3	crystallin, alpha B
Hspa8	10.16	7.42	1142	171	-6.7	heat shock 70kDa protein 8
Signaling						
Shcbp1	7.11	9.69	138	829	6.0	SHC SH2-domain binding protein 1
Adcy7	6.96	9.25	124	609	5.0	adenylate cyclase 7
Procr	10.78	9.14	1761	565	-3.1	protein C receptor, endothelial
Igf1bp4	10.46	8.81	1409	449	-3.2	insulin-like growth factor binding protein 4
Grb14	9.52	7.82	734	225	-3.2	growth factor receptor-bound protein 14
Snx12	10.85	9.01	1849	517	-3.6	sorting nexin 12
Ramp3	11.55	9.30	3007	629	-2.8	receptor (G protein-coupled) activity modifying protein 3
Appl2	11.20	8.67	2352	407	-5.9	adaptor protein, phosphotyrosine interaction, PH domain and leucine zipper containing 2
Rgs16	10.86	7.93	1859	244	-7.7	regulator of G-protein signaling 16
Transcription/Translation						
Krcc1	7.45	9.56	175	757	4.4	lysine-rich coiled-coil 1
Srsf1	8.41	10.40	341	1350	4.0	serine/arginine-rich splicing factor 1
Gatad2a	6.29	8.27	78	309	3.9	GATA zinc finger domain containing 2A
Srsf2	9.85	11.53	920	2962	3.2	serine/arginine-rich splicing factor 2
Hnrnpd	9.74	11.38	858	2674	3.1	heterogeneous nuclear ribonucleoprotein D (AU-rich element RNA binding protein 1, 37kDa)
Neat1	8.59	10.21	387	1186	3.1	nuclear paraspeckle assembly transcript 1 (non-protein coding)
Lmnb1	7.32	8.91	160	480	3.0	laminin B1
Malat1	10.59	8.91	1543	483	-3.2	metastasis associated lung adenocarcinoma transcript 1 (non-protein coding)
Taf1d	9.14	7.36	566	164	-3.4	TATA box binding protein (TBP)-associated factor, RNA polymerase I, D, 41kDa
Hnrpdl	12.03	10.23	4197	1203	-3.4	heterogeneous nuclear ribonucleoprotein D-like
Rpl41	8.37	6.56	330	94	-3.6	ribosomal protein L41
Luc7l	10.50	8.64	1448	398	-3.6	LUC7-like (S. cerevisiae)
Ccnl1	11.77	9.85	3500	922	-3.8	cyclin L1
Clk1	11.64	9.69	3199	825	-3.8	CDC-like kinase 1
Rps10	8.29	6.29	314	79	-4.0	ribosomal protein S10
Pabpc1	9.92	7.88	971	236	-4.2	poly(A) binding protein, cytoplasmic 1
Luc7l2	11.64	9.30	3185	632	-5.0	LUC7-like 2 (S. cerevisiae)
Txnip	10.11	7.41	1105	171	-7.1	thioredoxin interacting protein
Transport						
Chac2	6.77	8.65	109	403	3.7	ChaC, cation transport regulator homolog 2 (E. coli)
Slc22a4	9.90	8.25	955	304	-3.1	solute carrier family 22 (organic cation/zwitterion transporter), member 4
Slc35a2	8.95	7.28	493	156	-3.1	solute carrier family 35 (UDP-galactose transporter), member A2
Nptx1	9.53	7.84	737	229	-3.2	neuronal pentraxin I
Slc25a37	10.84	9.14	1830	565	-3.2	solute carrier family 25 (mitochondrial iron transporter), member 37

Supplementary Table 3. Gene expression in EO771/shCxc1. Shown are ≥ 3.0 -fold changes in gene expression with a raw score ≥ 300 in EO771/shCxc1 or EO771/Scr cells.

Function	log 2		Raw Score		FC	Gene Name
	Scr	shCxc1	Scr	shCxc1	sh/Scr	
Adhesion/ECM						
Plet1	9.07	7.15	538	142	-3.8	Placenta Expressed Transcript 1, ECM, wound repair
Apoptosis						
CD82	11.42	9.78	2747	878	-3.1	Kangai 1 (Suppression Of Tumorigenicity 6, Prostate
Immune/Inflammation						
Ly6a	12.93	11.29	7787	2512	-3.1	Lymphocyte antigen 6 complex, locus A, Stem cell antigen-1, Sca-1
Il23a	8.84	7.06	459	133	-3.5	Innate and adaptive immunity, autoimmunity, inflammatory cytokines
C3	8.48	6.55	358	94	-3.8	Complement Component 3, innate and adaptive immunity, inflammation
Cxcl1	11.06	9.07	2137	536	-4.0	Chemokine (C-X-C Motif) Ligand 1 (Melanoma Growth Stimulating Activity, Alpha)
CD68	8.62	6.54	394	93	-4.2	Macrophage phagocytosis
Invasion/Motility						
Plau	9.89	7.05	949	133	-7.3	Plasminogen activator urokinase
Mitosis						
Clip4	8.61	6.91	391	120	-3.6	CAP-GLY Domain Containing Linker Protein Family, Member 4, centrosome
Piwi2	9.46	7.64	707	199	-3.6	Piwi-Like RNA-Mediated Gene Silencing 2, meiosis, oncogene when overexpressed
Signaling						
Rgs16	10.79	9.15	1771	568	-3.2	Regulator of G-Protein Signaling 16
Transport						
Slc7a3	7.76	9.39	217	673	3.1	Solute Carrier Family 7 (Cationic Amino Acid Transporter, Y+ System), Member 3

Supplementary Table 4. Gene expression in EO771 isografts from SB25002-treated mice. Shown are genes with ≥ 3 -fold change in expression and a raw score ≥ 300 in mammary tumors from mice treated with vehicle or 20 mg/kg SB25002.

Function	log2		Raw Score		FC	Gene Name
	Vehicle	SB25002	Vehicle	SB25002		
Adhesion/ECM						
Cgref1	11.6121	13.3081	3130	10142	3.2	cell growth regulator with EF hand domain 1
Nrcam	8.0089	9.6418	258	799	3.1	neuronal cell adhesion molecule
Apoptosis						
Cidea	8.7618	7.1531	434	142	-3.0	cell death-inducing DNA fragmentation factor, alpha subunit-like effector A
Differentiation						
Krt18	13.0294	14.6218	8360	25211	3.0	keratin 18
Lor	9.5320	6.3053	740	79	-9.4	loricrin
Immune/Inflammation						
Ly6c1	14.9712	13.4000	32121	10809	-3.0	lymphocyte antigen 6 complex, locus C1
Ly6d	8.8947	7.3091	476	159	-3.0	lymphocyte antigen 6 complex, locus D
Tmem176a	10.6826	9.0431	1644	528	-3.1	transmembrane protein 176A
C1qtnf1	10.4737	8.6785	1422	410	-3.5	C1q and tumor necrosis factor related protein 1
Tmem176b	15.2836	13.2279	39886	9594	-4.2	transmembrane protein 176B
Invasion/Motility						
Tspan2	9.2743	10.8752	619	1878	3.0	tetraspanin 2
Tnnt2	9.8600	11.4300	929	2759	3.0	troponin T2, cardiac
Serpinb1a	12.8849	10.8336	7564	1825	-4.1	serine (or cysteine) peptidase inhibitor, clade B, member 1a
Metabolism						
Tex101	8.5414	10.3233	373	1281	3.4	testis expressed gene 101
Cpt1c	6.8928	8.5777	119	382	3.2	carnitine palmitoyltransferase 1c
Pla2g5	12.3834	10.8200	5343	1808	3.0	phospholipase A2, group V
Gsta2	8.9964	7.1455	511	142	-3.6	glutathione S-transferase, alpha 2 (Yc2)
Plin4	10.3196	7.7437	1278	214	-6.0	perilipin 4
Gpd1	9.8930	7.1120	951	138	-6.9	glycerol-3-phosphate dehydrogenase 1 (soluble)
Hp	14.7010	11.5504	26634	2999	-8.9	haptoglobin
Proliferation						
Figf	10.8829	9.3714	1888	640	3.0	c-fos induced growth factor
Greb1	12.9176	14.7121	7737	26840	3.5	gene regulated by estrogen in breast cancer protein
Signaling						
F3	9.0419	10.6820	527	1643	3.1	coagulation factor III
P2rx3	9.2673	7.6281	616	198	-3.1	purinergic receptor P2X, ligand-gated ion channel, 3
Snca	11.6458	9.5825	3204	767	-4.2	synuclein, gamma
Transcription/Translation						
Anp32a	12.4230	14.0442	5491	16894	3.1	acidic (leucine-rich) nuclear phosphoprotein 32 family, member A
Pcbd1	11.4736	9.7331	2844	851	-3.3	pterin 4 alpha carbinolamine dehydratase/dimerization cofactor of hepatocyte nuclear factor 1 alpha (TCF1) 1
Glod5	9.8789	7.7521	942	216	-4.4	glyoxalase domain containing 5
Transport						
Scara5	11.5306	9.7621	2958	868	-3.4	scavenger receptor class A, member 5 (putative)
Mup-ps16	9.3871	7.5667	670	190	-3.5	major urinary protein, pseudogene 16
Mup4	10.2305	8.1747	1201	289	-4.2	major urinary protein 4
Retn	9.6222	7.5379	788	186	-4.2	resistin
Mup19	11.7530	8.9928	3451	509	-6.8	major urinary protein 19

Supplemental Table 5. Gene expression in MC/Plac1 cells. Shown are genes with ≥ 3 -fold change in expression with a raw score ≥ 300 in MC/Ctl or MC/Plac1 cells.

	log2		Raw Score		FC	
Function	MC/Ctl	MC/Plac1	MC/Ctl	MC/Plac1	Plac1/Ctl	Gene Name
Adhesion/ECM						
Cldn1	8.07	10.78	269	1758	6.5	Claudin 1
Hs6st2	6.51	8.59	91	385	4.2	Heparan Sulfate 6-O-Sulfotransferase 2
Vcan	6.72	8.63	105	396	3.8	Versican
Lgals9	7.32	9.22	160	596	3.7	Lectin, Galactoside-Binding, Soluble, 9
Fn1	8.56	6.93	377	122	-3.1	Fibronectin 1
Plec	10.97	9.34	2006	648	-3.1	Plectin
Matn2	8.44	6.66	347	101	-3.4	Matrilin 2
Emp2	11.52	9.73	2937	849	-3.4	Epithelial membrane protein 2
Lrrc8a	8.5	6.54	362	93	-3.9	Leucine Rich Repeat Containing 8 Family, Member A
Differentiation						
Krt16	6.12	10.4	70	1351	19.4	Keratin 16
Fam198b	7.26	9.21	153	592	3.9	Family With Sequence Similarity 198, Member B
Sema3c	7.96	9.85	249	923	3.7	Sema Domain, Immunoglobulin Domain (Ig), Short Basic Domain, Secreted
Pard6g	8.22	9.89	298	949	3.2	Par-6 Family Cell Polarity Regulator Gamma
Scara5	9.28	7.64	622	199	-3.1	Scavenger Receptor Class A, Member 5
Cwh43	8.98	7.12	505	139	-3.6	Cell Wall Biogenesis 43 C-Terminal Homolog
Immune/Inflammation						
Cxcl11	5.25	10.46	38	1409	37.0	Chemokine (C-X-C Motif) Ligand 11
Iigp1	7.05	11.43	133	2759	21.0	Interferon inducible GTPase 1
Tgtp1	8.95	13.22	495	9541	19.3	T-cell specific GTPase 1
Cxcl10	7.27	10.98	154	2020	13.1	Chemokine (C-X-C Motif) Ligand 10
Ifi2712a	7.4	11.03	169	2091	12.4	Interferon, Alpha-Inducible Protein 27-Like 2
Irg1	6.19	9.74	73	855	11.7	Immunoresponsive 1 Homolog (Mouse)
Trim30a	8.62	11.99	393	4068	10.5	Tripartite Motif Containing 5
Gbp6	7.9	11.24	239	2419	10.1	Guanylate Binding Protein Family, Member 6
Ifit3	9.91	13.22	962	9541	9.9	Interferon-Induced Protein With Tetratricopeptide Repeats 3
Zbp1	7.68	10.8	205	1783	8.8	Z-DNA Binding Protein 1
Rsad2	9.62	12.7	787	6654	8.6	Radical S-Adenosyl Methionine Domain Containing 2
Ifit1	10.63	13.62	1585	12590	7.9	Interferon-Induced Protein With Tetratricopeptide Repeats 1
Gbp3	10.39	13.22	1342	9541	7.1	Guanylate Binding Protein 3
Ccl5	10.87	13.69	1872	13216	7.1	Chemokine (C-C Motif) Ligand 5
Ddx60	8.53	11.35	370	2610	7.1	DEAD (Asp-Glu-Ala-Asp) Box Polypeptide 60
Irf7	8.59	11.4	385	2702	7.0	Interferon Regulatory Factor 7
Il33	6.21	8.64	74	399	5.4	Interleukin-33
Oasl2	9.92	12.29	969	5008	5.2	2'-5'-Oligoadenylate Synthetase-Like
H2-Q7	6.63	8.94	99	491	5.0	Histocompatibility 2, Q region locus 7
Ifit2	10.32	12.6	1278	6208	4.9	Interferon-Induced Protein With Tetratricopeptide Repeats 2
Ifi44	10.03	12.28	1046	4973	4.8	Interferon-Induced Protein 44
Ccl2	7.52	9.75	184	861	4.7	Chemokine (C-C Motif) Ligand 2
Usp18	10.98	13.2	2020	9410	4.7	Ubiquitin Specific Peptidase 18
Isg15	11.38	13.56	2665	12077	4.5	ISG15 Ubiquitin-Like Modifier
Dhx58	7.63	9.73	198	849	4.3	DEXH (Asp-Glu-X-His) Box Polypeptide 58
Igtp	10.94	12.95	1965	7913	4.0	Interferon gamma induced GTPase
Gbp2	11.13	12.98	2241	8079	3.6	Guanylate Binding Protein 2, Interferon-Inducible
Ifih1	10.17	11.94	1152	3929	3.4	Interferon Induced With Helicase C Domain 1
Ifi47	10.92	12.69	1938	6608	3.4	Interferon gamma inducible protein 47
Irgm1	11.47	13.2	2837	9410	3.3	Immunity-related GTPase
Lrr1	7.12	8.83	139	455	3.3	Leucine Rich Repeat Protein 1
Cd274	7.35	8.94	163	491	3.0	Programmed Cell Death 1 Ligand 1
Oasl1	8.03	9.69	261	826	3.2	2'-5'-Oligoadenylate Synthetase-Like1
Gbp7	9.52	11.17	734	2304	3.1	Guanylate Binding Protein 7
Aebp1	9.79	11.43	885	2759	3.1	Adipocyte Enhancer Binding Protein 1
Oas1a	11.21	12.81	2369	7181	3.0	2'-5'-Oligoadenylate Synthetase 1, 44/46kDa
Cxcl2	9.38	7.69	666	207	-3.2	Chemokine (C-X-C Motif) Ligand 2
Cd68	10.49	8.48	1438	357	-4.0	Scavenger Receptor Class D, Member 1
Il1a	8.44	5.93	347	61	-5.7	Interleukin 1, Alpha
Invasion/Motility						
Fhod3	5.32	9.92	40	969	24.3	Formin Homology 2 Domain Containing 3
Serpinb2	5.20	9.30	37	630	17.1	Serpin Peptidase Inhibitor, Clade B (Ovalbumin), Member 2
Plat	7.68	9.68	205	820	4.0	Plasminogen Activator, Tissue
Pfn2	7.82	9.77	226	873	3.9	Profilin 2
Myo10	9.93	11.63	976	3169	3.3	myosin X
Psmb9	9.68	11.42	820	2740	3.3	Proteasome (Prosome, Macropain) Subunit, Beta Type, 9
Hmmr	7.89	9.54	237	744	3.2	Hyaluronan-Mediated Motility Receptor
Malat1	12.05	10.16	4240	1144	-4.0	Metastasis Associated Lung Adenocarcinoma Transcript 1
Tnfrsf2	10.8	8.69	1783	413	-4.3	Tumor Necrosis Factor, Alpha-Induced Protein 2
Mmp3	9.06	6.9	534	119	-4.5	Matrix Metallopeptidase 3 (Stromelysin 1)
Ctsc	8.72	6.48	422	89	-4.7	Cathepsin C
Mmp10	10.39	7.88	1342	236	-5.7	Matrix Metallopeptidase 10 (Stromelysin 2)
Metabolism						
Cmpk2	7.56	10.03	189	1046	5.9	CMP (UMP-CMP) Kinase 2, Mitochondrial
Cyp11b1	7.84	9.98	229	1010	4.6	Cytochrome P450, Family 1, Subfamily B, Polypeptide 11
Ugt1a1	9.91	11.59	962	3083	3.2	UDP Glucuronosyltransferase 1 Family, Polypeptide A1
Ckb	10.01	8.41	1031	340	-3.0	Creatine kinase, brain
Pck2	10.36	8.67	1314	407	-3.2	Phosphoenolpyruvate Carboxykinase 2
Shmt2	10.48	8.85	1428	461	-3.1	Serine Hydroxymethyltransferase 2 (Mitochondrial)
Mthfd2	11.21	9.48	2369	714	-3.2	Methylenetetrahydrofolate Dehydrogenase (NADP+ Dependent) 2

Psph	12.25	10.51	4871	1458	-3.4	Phosphoserine Phosphatase1
Aldoc	10.29	8.63	1252	396	-3.6	Aldolase C, Fructose-Bisphosphate
Stbd1	11.22	9.37	2385	662	-3.6	Starch Binding Domain 1
Ero1l	11.6	9.65	3104	803	-3.7	Endoplasmic Oxidoreductin-1-Like Protein
Aspa	10.03	8.07	1046	269	-3.9	Aspartoacylase
Acot2	8.52	6.52	367	92	-4.0	Acyl-CoA Thioesterase 2
Gpt2	10.54	10.22	1489	1193	-4.0	Glutamic Pyruvate Transaminase
Pycr1	9.5	7.49	724	180	-4.0	Pyrraline-5-Carboxylate Reductase 1
Hmox1	12.11	10.07	4421	1075	-4.1	Heme Oxygenase (Decycling) 1
Acsbg1	8.56	6.44	377	87	-4.3	Acyl-CoA Synthetase Bubblegum Family Member 1
Cth	9.87	7.55	936	187	-5.0	Cystathionine Gamma-Lyase
Gsta1/Gsta2	11.5	7.27	2896	154	-16.7	Glutathione S-Transferase Alpha 1/Alpha 2
Inmt	11.59	6.63	3083	99	-31.3	Indolethylamine N-Methyltransferase
Mitosis						
Kif20a	8.35	10.35	326	1305	4.0	Kinesin Family Member 20A1
Nusap1	8.07	10.06	269	1067	4.0	Nucleolar And Spindle Associated Protein 1
Plk1	7.52	9.35	184	653	3.6	Polo-like Kinase 1
Ttk	7.18	9.01	145	516	3.6	TTK Protein Kinase
Kif23	6.93	8.7	122	416	3.4	Kinesin Family Member 23
Prc1	8.62	10.36	393	1314	3.4	Protein Regulator Of Cytokinesis 1
Aurkb	7.83	9.55	228	750	3.3	Aurora B Kinase
Kif2c	8.09	9.8	272	891	3.3	Kinesin Family Member 2c
Aspm	7.57	9.25	190	609	3.2	Asp (Abnormal Spindle) Homolog, Microcephaly Associated
Zwilch	8.05	9.73	265	849	3.2	Zwilch Kinetochore Protein
Ncapg	7.26	8.92	153	484	3.2	Non-SMC Condensin I Complex, Subunit G
Birc5	9.69	11.34	826	2592	3.1	Baculoviral IAP Repeat Containing 5
Mastl	6.62	8.26	98	307	3.1	Microtubule Associated Serine/Threonine Kinase-Like
Kif22	7.1	8.72	137	422	3.1	Kinesin Family Member 22
Nuf2	7.54	9.17	186	576	3.1	NUF2, NDC80 Kinetochore Complex Component
Cenpe	8.28	9.87	311	936	3.0	Centromere protein E
Fam110c	9.45	7.83	699	228	-3.1	Family With Sequence Similarity 110, Member C
Proliferation						
Plac1	7.51	11.37	182	2647	14.5	Placental-specific 1
Shcbp1	8.21	10.16	296	1144	3.9	SHC SH2-Domain Binding Protein 11
Wnt4	8.42	10.2	343	1176	3.4	Wingless-Type MMTV Integration Site Family, Member 4
Rab32	8.22	10.09	298	1090	3.7	RAB32, Member RAS Oncogene Family
Afp	6.4	8.23	84	300	3.6	Alpha-fetoprotein
Mertk	6.55	8.29	94	313	3.3	C-Mer Proto-Oncogene Tyrosine Kinase
Ccna2	8.84	10.53	458	1479	3.2	Cyclin A2
Smpd13b	8.33	9.97	322	1003	3.1	Sphingomyelin Phosphodiesterase, Acid-Like 3B1
Ghr	9.88	11.52	942	2937	3.1	Growth hormone receptor
Bnip3	11.61	9.96	3126	996	-3.1	BCL2/Adenovirus E1B 19kDa Interacting Protein 3
Trib3	11.13	9.25	2241	609	-3.6	Tribbles Pseudokinase 3
Gas5	9.82	7.91	904	241	-3.8	Growth Arrest-Specific 5
Phlda2	9.71	7.75	838	215	-3.9	Pleckstrin Homology-Like Domain, Family A, Member 2
Vegfa	11.76	9.67	3468	815	-4.2	Vascular endothelial growth factor A
Areg	11.03	8.94	2091	491	-4.3	Amphiregulin
Reep6	10.85	8.69	1846	413	-4.5	Receptor Accessory Protein 6
Csf1r	9.98	7.78	1010	220	-4.6	Colony Stimulating Factor 1 Receptor
Prkg2	11.34	9.11	2592	553	-4.7	Protein Kinase, CGMP-Dependent, Type II
Artn	9.45	7.15	699	142	-4.9	Artemin
Ndrp1	11.85	9.48	3692	714	-5.0	N-Myc Downstream Regulated 1
Chac1	11.53	9.02	2957	519	-5.7	ChaC, Cation Transport Regulator Homolog 1
Fgf21	8.46	5.95	352	62	-5.7	Fibroblast growth factor 21
Fam129a	9.37	6.76	662	108	-6.1	Family With Sequence Similarity 129, Member A
Secretion						
Inhbb	8.76	11.76	434	3468	8.0	Activin Beta-B Chain
Fst	7.18	9.81	145	898	6.2	Follistatin
Tac1	7.03	8.91	131	481	3.7	Tachykinin, Precursor 1
Transport						
Rtp4	7.03	8.84	131	458	3.5	Receptor (Chemosensory) Transporter Protein
Abca1	8.81	10.5	449	1448	3.2	ATP-Binding Cassette, Sub-Family A (ABC1), Member 1
Slc1a4	9.29	7.59	626	193	-3.2	Solute Carrier Family 1 (Glutamate/Neutral Amino Acid Transporter), Member 4
Fxyd2	10.25	8.26	1218	307	-4.0	FXD Domain Containing Ion Transport Regulator 2
Slc7a11	8.84	5.84	458	57	-8.0	Solute carrier family 7 (anionic amino acid transporter light chain, xc-system), member 11
Transcription/Translation						
Hist1h2b	8.77	12.55	437	5997	13.9	Histone cluster 1, H2b
Cspsr	5.81	8.28	56	311	5.9	Component of Sp100-rs
Gadd45g	9.95	12.36	989	5257	5.3	Growth Arrest And DNA-Damage-Inducible, Gamma
Hist1h3b	6.22	8.58	75	383	5.1	Histone cluster 1, H3b
Hist1h4a	6.16	8.3	72	315	4.6	Histone cluster 1, H4a
Hopx	7.44	9.53	174	739	4.3	HOP Homeobox
Depdc1a	7.35	9.26	163	613	3.8	DEP Domain Containing 1
Foxm1	6.6	8.45	97	350	3.6	Forkhead Box M1
Hist2h2aa	8.44	10.23	347	1201	3.5	Histone cluster 2, H2aa
Nr4a2	7.12	8.92	139	484	3.5	Nuclear Receptor Subfamily 4, Group A, Member 2
Stat1	9.86	11.59	929	3083	3.3	Signal transducer and activator of transcription 1, 91kDa
Atxn7l1	7.07	8.8	134	446	3.3	Ataxin 7-Like 1
Id3	9.42	11.09	685	2180	3.2	Inhibitor of DNA binding 3, dominant negative helix-loop-helix protein
Sp100	7.39	9.02	168	519	3.1	SP100 Nuclear Antigen
Txnip	10.35	8.65	1305	402	-3.2	Thioredoxin Interacting Protein
Rpl30	8.36	6.51	329	91	-3.6	Ribosomal Protein L30

Supplementary Table 6. List of primers for qRT-PCR analysis

Gene Accession #	Primer Name	Sequence	Amplicon size (bp)	Primer Location
Cxcl1 NM_008176.3	mCxcl1 rRNA-F mCxcl1 rRNA-R	GTGTCTAGTTGGTAGGGCATAAT CAGTCCTTTGAACGTCTCTGT	94	823-846 896-917
Ccl2 NM_011333.3	mCcl2 rRNA-F mCcl2 rRNA-R	CTCGGACTGTGATGCCTTAAT TGGATCCACACCTTGCAATTA	106	538-559 623-644
Ccl5 NM_013653.3	mCcl5 rRNA-F mCcl5 rRNA-R	CCAGAGAAGAAGTGGGTTCAAG AGCAATGACAGGGAAGCTATAC	100	283-305 361-383
Ccl7 NM_013654.3	mCcl7 rRNA-F mCcl7 rRNA-R	GGATAGGAGCTGTCTGTAGGA CATGAGGTCTCCAGAGCTTTAC	128	472-493 578-600
CD274 NM_021893.3	mCD274 rRNA-F mCD274 rRNA-R	GAGTGCAGATTCCTGTAGAAC CTCCTCTCCTGCCACAAAC	99	198-220 227-297
Lif NM_008501.2	mLif rRNA-F mLif rRNA-R	CGCCAATGCTCTCTTCATTTT ATGGGAAGTCTGTCATGTTAGG	98	177-198 253-275
Plac1 NM_019538.4	mPlac1 rRNA-F mPlac1 rRNA-R	GAGGTCCTTCTTGTGTAGTCATC ATCTGGGCACTATATGGGTTTC	96	790-813 864-886
18S rRNA NR_003278	m18S rRNA-F m18S rRNA-R	TCGGAACTGAGGCCATGATT CCTCCGACTTTTCGTTCTTGATT	146	900-919 1024-1045
CD68 NM_001291058.1	mCD68 rRNA-F mCD68 rRNA-R	CCCACCTGTCTCTCTCATTTT GTATTCCACCGCCATGTAGT	107	545-566 632-652
Ly6a NM_001271416.1	mLy6a rRNA-F mLy68 rRNA-R	CTCAGGAGGCAGCAGTTATT GTACCCAGGATCTCCATACTTTC	106	164-184 247-270
IL23a NM_031252.2	mIL23a rRNA-F mIL23a rRNA-R	CCAGCGGGACATATGAATCTAC TGTGGGTCAACAACCATCTTC	95	148-170 223-243
Plau NM_008873.3	mPlau rRNA-F mPlau rRNA-R	GATTCTGGAGGACCGCTTATC GTAGACACCGGGCTTGTTT	105	1129-1150 1215-1234